Diel fluctuations in *in-vivo* SnRK1 activity in Arabidopsis rosettes during light-dark cycles

Omri Avidan[1], Thiago A. Moraes[1, a], Virginie Mengin[1, b], Regina Feil[1], Filip Rolland[2,3], Mark Stitt[1,*] and John E. Lunn[1,*]

[1]Max Planck Institute of Molecular Plant Physiology, Am Muehlenberg 1, 14476 Potsdam-Golm, Germany

[2]Laboratory of Molecular Plant Biology, KU Leuven, Leuven, Belgium

[3] KU Leuven Plant Institute (LPI), Leuven, Belgium

*Authors for correspondence: mstitt@mpimp-golm.mpg.de, lunn@mpimp-golm.mpg.de

[a]Current address: Crop Science Centre, Lawrence Weaver Road, Cambridge CB3 0LE, UK

[b]Current address: Department of Biological Sciences, University of Essex, Colchester, CO4 3SQ, UK.

ORCID

OA: 0000-0002-1844-1280 (avidan@mpimp-golm.mpg.de)

TAM: 0000-0002-7156-6947 (ta507@cam.ac.uk)

VM: 0000-0002-4958-4209 (v.mengin@essex.ac.uk)

RF: 0000-0002-9936-1337 (feil@mpimp-golm.mpg.de)

FR: 0000-0003-2601-0752 (filip.rolland@kuleuven.be)

MS: 0000-0002-4900-1763 (mstitt@mpimp-golm.mpg.de)

JEL: 0000-0001-8533-3004 (lunn@mpimp-golm.mpg.de)

Running Title: Diel fluctuations in SnRK1 activity in leaves

One sentence summary: *In vivo* SnRK1 activity shows an unexpected diel response and a complex relationship with trehalose 6-phosphate and other possible metabolic regulators.

Abstract

SUCROSE-NON-FERMENTING1 (SNF1)-RELATED KINASE1 (SnRK1) is a central hub in carbon and energy signalling in plants, and is orthologous with SNF1 in yeast and the AMP-ACTIVATED PROTEIN KINASE (AMPK) in animals. Previous studies of SnRK1 relied on *in-vitro* activity assays or on monitoring the expression of putative marker genes. Neither approach gives unambiguous information about *in-vivo* SnRK1 activity. We have monitored *in-vivo* SnRK1 activity using Arabidopsis (*Arabidopsis thaliana*) reporter lines that express a chimeric polypeptide with a SNF1/SnRK1/AMPK-specific phosphorylation site. We investigated responses during an equinoctial diel cycle, and after perturbing this cycle. As expected, *in vivo* SnRK1 activity rose towards the end of the night and rose even further when the night was extended. Unexpectedly, although sugars rose after dawn, SnRK1 activity did not decline until about 12 hours into the light period. The sucrose signal trehalose 6-phosphate (Tre6P) has been shown to inhibit SnRK1 *in vitro*. We introduced the SnRK1 reporter into lines that harboured an inducible *TREHALOSE-6-PHOSPHATE SYNTHASE* construct. Elevated Tre6P decreased *in-vivo* SnRK1 activity in the light period, but not at the end of the night. Reporter polypeptide phosphorylation was sometimes negatively correlated with Tre6P, but a stronger and more widespread negative correlation was observed with glucose 6-phosphate. We propose that SnRK1 operates within a network that controls carbon utilization and maintains diel sugar homeostasis, and that Tre6P, hexose phosphates and the circadian clock contribute to regulation of SnRK1 activity in a context-dependent manner, and SnRK1-signalling is further modulated by factors that act downstream of SnRK1.

Keywords: *Arabidopsis thaliana*, SnRK1, trehalose 6-phosphate, glucose 6-phosphate, diel, circadian clock, starch

Abbreviations: GEN, general SnRK1 reporter; Glc1P, glucose 1-phosphate; Glc6P, glucose 6-phosphate; NUC, nuclear SnRK1 reporter; SnRK1, SUCROSE-NON-FERMENTING1-RELATED KINASE1; TPP, trehalose-6-phosphate phosphatase; TPS, trehalose-6-phosphate synthase; Tre6P, trehalose 6-phosphate; UDP-Glc, UDP-glucose.

54 **Introduction**

55 Plant SUCROSE-NON-FERMENTING1-RELATED PROTEIN KINASES 1 (SnRK1) belongs to a eukaryotic
56 family of Ca^{+2}-independent Ser/Thr protein kinases. SnRK1 is implicated in maintaining cellular
57 homeostasis and energy balance alongside linking carbon (C) availability and growth, and has been
58 extensively studied in recent years (Polge and Thomas, 2006; Jossier *et al.*, 2009; Hulsmans *et al.*,
59 2016; Baena-González *et al*., 2007; Paul *et al.*, 2018; 2020; Crepin and Rolland, 2019; Baena-González
60 and Lunn, 2020). These functions are broadly similar to those observed for its yeast and animal
61 orthologues, SUCROSE-NON-FERMENTING1 (SNF1) and AMP-ACTIVATED PROTEIN KINASE (AMPK) but
62 our understanding of the functions and regulation of SnRK1 in plants is much less complete.

63 SnRK1 is a heterotrimer consisting of a catalytic (α) subunit and two regulatory (β and βγ)
64 subunits that modify complex stability, activity, interactions and cellular localization (Polge *et al.*,
65 2008; Nietzsche *et al.*, 2016; Wang *et al.*, 2020). It is located in the nucleus and cytosol (Nietzsche *et*
66 *al.*, 2014; Blanco *et al.*, 2019; Ramon *et al.*, 2019) and has also been reported to be present in plastids
67 (Ávila-Castañeda *et al.*, 2014; Ruiz-Gayosso *et al.*, 2018). According to current knowledge, the mode
68 of regulation differs from that of SNF1 and AMPK. The regulatory properties of these kinases have
69 been studied mainly by *in-vitro* assays, which monitor phosphorylation of peptides containing an
70 evolutionarily conserved SNF1/SnRK1/AMPK-specific recognition sequence:
71 [MLVFI].X.[RKH].X.X.**S**.X.X.X.[LFIMV] or the less favoured [MLVFI].[RKH].X.X.X.**S**.X.X.X.[LFIMV] (Dale *et*
72 *al.*, 1995). Such studies have demonstrated that animal AMPK, and to a certain degree also yeast SNF1,
73 are directly regulated by AMP and/or ADP (Hardie and Carling, 1997; Hardie *et al.*, 1998; Mayer *et al.*,
74 2011). In mammals, these adenylates inhibit T-loop dephosphorylation, thereby activating the
75 catalytic (α) subunit in low energy conditions and/or in response to low C availability (García-Salcedo
76 *et al.*, 2014; Crozet *et al.*, 2014). In contrast, plant SnRK1 is not activated by adenylates in *in-vitro*
77 assays. Instead, it is inhibited *in vitro* by sugar phosphates, such as trehalose 6-P (Tre6P), glucose 6-
78 phosphate (Glc6P) and glucose 1-phosphate (Glc1P) (Toroser *et al.*, 2000; Lu *et al.*, 2007; Zhang *et al.*,
79 2009; Emanuelle *et al.*, 2015; Broeckx *et al.*, 2016; Zhai *et al.*, 2017; 2018; Ruiz-Gayosso *et al.*, 2018).
80 Inhibition by sugar phosphates could potentially link SnRK1 activity to C availability rather than energy
81 status (Hara *et al.*, 2013; Nunes *et al.*, 2013; Herzig and Shaw, 2017). These *in-vitro* studies also
82 indicated that inhibition by Tre6P requires an unknown proteinaceous factor that is present in growing
83 tissues but not in mature source leaves (Toroser *et al.*, 2000; Zhang *et al.*, 2009; Emanuelle *et al.*,
84 2015). Subsequent studies have shown that Tre6P can bind directly to the SnRK1 catalytic α subunit,
85 thereby interfering with binding of the SnRK1-activating kinases GRIK1/2, leading to inhibition of
86 SnRK1 activity (Glab *et al.*, 2017; Zhai *et al.*, 2018; Hwang et al., 2019). However, GRIK1/2 might not
87 be the only mechanism by which Tre6P inhibits SnRK1 activity. As GRIK1/2 are widely expressed in

88 source leaves, Zhai et al. (2018) concluded that they were unlikely to be the unknown proteinaceous
89 factor from young tissues that was referred to by Zhang et al. (2009).

90 Glc6P and Glc1P are intermediates in glycolysis, gluconeogenesis and in the synthesis and
91 degradation of major carbohydrate reserves like starch and sucrose. Tre6P is an intermediate in the
92 pathway of trehalose biosynthesis. It is synthesized from UDP-Glc and Glc6P by TREHALOSE-6-
93 PHOSPHATE SYNTHASE (TPS) and is dephosphorylated to trehalose by TREHALOSE-6-PHOSPHATE
94 PHOSPHATASE (TPP) (Cabib and Leloir, 1958). Trehalose is a major C storage metabolite, osmolyte and
95 stress protectant in fungi, but has been largely replaced by sucrose in vascular plants, allowing neo-
96 functionalization of the trehalose biosynthesis pathway (Goddijn and van Dun, 1999; Lunn *et al.*, 2014;
97 Lunn, 2016). In addition to catalytically active class I TPS proteins), plants possess a large family of
98 catalytically inactive class II TPS proteins (Leyman *et al*., 2001; Harthill *et al.*, 2006; Lunn, 2007;
99 Vandesteene *et al.*, 2010; Lunn et al., 2014; Delorge *et al.*, 2015) as well as a large family of TPP
100 proteins (Leyman *et al*., 2001; Vandesteene *et al.*, 2012; Kretzschmar *et al.*, 2015). Tre6P is considered
101 to serve as a signal of sucrose availability (Lunn *et al.*, 2006), acting to regulate C allocation between
102 sucrose and other photosynthesis products in source leaves, and to link sucrose supply and growth in
103 sink organs (Schluepmann *et al.*, 2003; Martins *et al.*, 2013; Wahl *et al.*, 2013; Figueroa *et al.*, 2016;
104 Paul *et al.*, 2018; 2020; Fichtner and Lunn, 2021).

105 The possible contribution of Glc6P and Glc1P to regulation of SnRK1 activity *in planta* has not
106 been addressed in detail. Interactions between Tre6P and SnRK1 have been more extensively studied,
107 mainly by investigating changes in SnRK1 marker transcript abundance (Zhang *et al.*, 2009; 2015;
108 Henry *et al.*, 2015; Bledsoe *et al.*, 2017) and post-translational regulation of target enzymes Baena-
109 González and Sheen, 2008; Figueroa *et al.*, 2016). The former builds on the work of Baena-González
110 *et al*. (2007) who, using a protoplast overexpression system, identified over 1000 genes as
111 downstream targets of SnRK1, such as *DIN6*, *DIN1*, *BCAT2* and *EXP10*, whose expression is regulated
112 by SnRK1-mediated phosphorylation of upstream transcription factors, such as bZIP11 (Ma et al.,
113 2011) and bZIP63 (Mair et al., 2016). Their expression has been widely used as a sensitive readout of
114 SnRK1 activity, either via promoter activation assays (Rodrigues *et al.*, 2013; Ramon *et al.*, 2019) or by
115 analyses of transcript abundance. Abundance of SnRK1-induced transcripts is typically low in a diel
116 cycle but rises strongly when plants are starved by transfer to continuous darkness (Baena-González
117 *et al.*, 2007; Baena-González and Sheen, 2008; Usadel *et al.*, 2008; Flis *et al*., 2016) as expected if
118 SnRK1 is activated in C starvation conditions (Mair *et al.*, 2015; Pedrotti *et al.*, 2018; Ramon *et al.*,
119 2019). Their abundance often changes reciprocally to Tre6P levels in starvation treatments and other
120 perturbations in several species and tissues (Martínez-Barajas *et al.*, 2011; Wingler *et al.*, 2012; Nunes
121 *et al.*, 2013; Henry *et al.*, 2015; Nuccio *et al.*, 2015; Baena-González and Lunn, 2020; Peixoto *et al.*,

122 2021) providing correlative evidence for the idea that Tre6P inhibits SnRK1 *in vivo*. Application of
123 permeable Tre6P analogues to Arabidopsis led to changes in transcript abundance for a subset of
124 these SnRK1 downstream target genes that were consistent with Tre6P acting to inhibit SnRK1
125 (Griffiths *et al*., 2016). Further support for partial convergence of the SnRK1 and Tre6P signalling
126 pathways was provided by the identification of several class II TPSs as transcriptional and post-
127 translational SnRK1 targets (Glinski and Weckwerth, 2005; Harthill *et al*., 2006; Cho *et al.*, 2016;
128 Nukarinen *et al.*, 2016). However, the functional significance of this observation remains unclear
129 because the precise role of the TPS class II proteins has not yet been defined (Schluepmann and Paul,
130 2009; Ponnu *et al*., 2011; Yang *et al.*, 2012; Lunn et al. 2014; Delorge *et al.*, 2015; Figueroa and Lunn,
131 2016). More recently, it was demonstrated that mutant lines with increased or reduced expression of
132 SnRK1 exhibit an altered relationship between sucrose and Tre6P in diel cycles, as well as modified
133 anaplerotic flux of carbon to the tricarboxylic acid cycle that is reminiscent of responses to Tre6P
134 (Peixoto *et al.*, 2021). Furthermore, mutations in the *SnRK1α1* and *SnRK1βγ* genes were shown to
135 suppress developmental defects in the Arabidopsis *tps1* mutant (Zacharaki *et al*., 2022).

136 Taken together, these results point to SnRK1 and Tre6P signalling being closely intertwined.
137 They also indicate that SnRK1 signalling is involved not only in starvation responses, but also in the
138 coordination of metabolism in benign conditions where plants are not C-starved or facing a large C
139 excess (see also Baena-González and Lunn, 2020). However, many open questions remain; for
140 example, negative correlations between Tre6P levels and the transcript abundance of SnRK1-induced
141 genes are seen in mature tissues even though Tre6P does not inhibit SnRK1 activity in *in-vitro* assays
142 with material from mature tissues (see above and Baena-González and Lunn, 2020). Moreover, there
143 is an inconsistent correlation between Tre6P levels and transcript abundance of SnRK1 target genes
144 in *in-vitro* cultured excised maize kernels (Bledsoe *et al.*, 2017, see also Baena-González and Lunn,
145 2020). It remains possible that Tre6P also acts on signalling downstream of SnRK1, as is the case in
146 yeast (Deroover *et al*., 2016), resulting in changes in downstream transcript abundance that are not
147 directly due to inhibition of SnRK1 itself. Interpretation is further complicated by potential interactions
148 between SnRK1 and TARGET OF RAPAMYCIN (TOR) signalling (Lastdrager *et al.*, 2014; Margalha and
149 Confraria, 2019; Ryabova *et al*., 2019).

150 The two main approaches employed in plants to study SnRK1 regulation have shortcomings
151 which have not been addressed to date. The *in-vitro* assay is direct and highly specific, but the use of
152 crude extracts or purified proteins may bring about other complications due to loss of the *in-vivo*
153 context, such as artificial interactions or potential loss of regulatory elements that otherwise would
154 have an effect on activity (Baena-González and Lunn, 2020). Monitoring changes in expression of
155 SnRK1 marker genes is sensitive, but gene expression is an indirect readout that may be prone to

156 secondary effects that are unrelated to SnRK1 activity. Indeed, there is often poor agreement between
157 SnRK1 activity in the *in-vitro* phosphorylation assay and changes in SnRK1 target gene expression
158 (Debast *et al.*, 2011; Martínez-Barajas *et al.*, 2011; Baena-González and Lunn, 2020).

159 Working in yeast, Deroover *et al.* (2016) developed a specific *in-vivo* SNF1 reporter that
160 harbours an SNF1/SnRK1/AMPK-specific recognition sequence-containing peptide, based on rat
161 ACETYL COA CARBOXYLASE 1 (ACC1), an established AMPK target (Dale *et al.*, 1995). The
162 phosphorylation status of this peptide can be monitored by extraction and immunoblot analysis with
163 a validated commercial phospho-specific antibody, providing a direct measure of *in-vivo* SNF1 activity.
164 Subsequently, modified ACC1 reporters were used in Arabidopsis to study the regulation of SnRK1
165 activity by nitrogen status (Sanagi *et al.*, 2021) and in other responses (Muralidhara *et al*.,
166 2021;cHenninger *et al*., 2022; Belda-Palazon *et al*., 2022).

167 We have used Arabidopsis ACC1 reporter lines to investigate *in-vivo* SnRK1 activity during a
168 diel cycle in benign conditions, when the C supply is only slightly restricting growth, and after changing
169 the light regime to modify the C supply. We have also introduced the reporter construct into
170 Arabidopsis lines in which Tre6P levels can be increased in an inducible manner (Martins *et al*., 2013;
171 Figueroa *et al*., 2016). We show that SnRK1 activity does not change reciprocally to overall C
172 availability, with a peak at dawn and a minimum at dusk. Instead, SnRK1 activity appears to be
173 maintained in the light period, declines after darkening and rises towards the end of the night.
174 Furthermore, SnRK1 activity *in vivo* is not strongly or consistently inhibited by an induced increase in
175 Tre6P. Multiple regression analyses of metabolite levels indicate that the link between *in-vivo* SnRK1
176 activity and the level of Tre6P is context-dependent and point to SnRK1 activity being regulated *in vivo*
177 by additional mechanisms, including inhibition by Glc6P.

178

179 **Results**

180 *Reporter constructs to quantify* in vivo *SnRK1 activity*

181 To obtain a direct *in-vivo* readout of SnRK1 activity in Arabidopsis we employed transgenic SnRK1-
182 reporter lines expressing a peptide derived from the Ser79 phosphorylation site of ACC1 fused to
183 GREEN FLUORESCENT PROTEIN (GFP), which was used to normalize for the level of expression of the
184 reporter polypeptide (see Supplementary Figure S1 for full description) and to monitor its localization
185 (see below). The level of phosphorylation of the ACC1 peptide (pACC) was assessed using a specific
186 anti-phospho-site antibody, and an anti-GFP antibody was used to normalize for expression level and
187 gel loading. To increase statistical and biological robustness, we used three-four biological replicates
188 per time point. An additional control sample (extended night) was loaded in all gels, and used to

189 correct for between-gel variation. We took the normalized pACC/GFP signal ratio as a readout of *in-*
190 *vivo* SnRK1 activity at a given time point (for details see Methods and Supplementary Figure S1).
191 Two transgenic lines were used: (i) expressing a nuclear reporter (NUC), that contains the SV40
192 nuclear location signal (NLS) and (ii) expressing a general reporter (GEN), in which GFP is observed in
193 both the nucleus and the cytoplasm (Supplementary Figure S2).
194
195 *Validation of the reporter construct in Arabidopsis rosettes*
196 The specificity of the ACC1 reporter peptide was previously tested in yeast by incubating WT and *snf1*
197 mutant cells with fermentable glycerol and ethanol to induce SNF1 or with glucose to inhibit SNF1
198 activity (Deroover *et al.*, 2016). The peptide was phosphorylated under fermenting conditions but not
199 following glucose addition in the wild type background, while no phosphorylation was observed in the
200 *snf1* background, suggesting that the reporter is indeed SNF1-specific in yeast. Sanagi *et al.* (2021)
201 validated an ACC1-based SnRK1 reporter in Arabidopsis mesophyll protoplasts, by showing that
202 phosphorylation is increased by transient expression of wild-type SnRK1α1 but not by expression of a
203 mutated form, SnRK1α1^{K48A}, which is defective in the SnRK1 ATP-binding pocket (K48M). They also
204 showed that there is less phosphorylation in protoplasts prepared from inducible *snrk1α* knockdown
205 plants than in protoplasts prepared from wild-type plants.
206 We took two approaches to further validate the reporters for use in whole Arabidopsis
207 rosettes. In the first approach, we subjected GEN and NUC lines to 3-h of extended darkness, starting
208 at the end of the night (Supplementary Figure S3A; Supplementary Dataset S1 – Exp.1). Extended
209 darkness is known to activate SnRK1 (see Introduction). As expected, phosphorylation of both
210 reporters increased in extended darkness, with phosphorylation being significantly higher at ZT25
211 (zeitgeber time, i.e. 25 h after the previous dawn and into the extended night) and rising further at
212 ZT27 in NUC, and being significantly higher by ZT27 in GEN. In the second approach, the NUC reporter
213 was crossed to a 35:SnRK1α1 line that has elevated SnRK1 activity and to the 35S:SnRK1α1^{K48M} line
214 expressing a catalytically inactive mutant protein (Jossier *et al.*, 2009; Crozet *et al*., 2014; Cho *et al.*,
215 2016) (Supplementary Figure S3B; Supplementary Dataset S1 – Exp.2). The crossed lines and a NUC
216 control were grown in equinoctial growth conditions for 22 days after sowing (DAS), and then
217 harvested at ZT0, 8, 16, 24 and 28 (i.e. 4-h of extended darkness). We confirmed expression of SnRK1
218 proteins in these lines by immunoblotting with anti-SnRK1α1 antibody (Supplementary Figure S3C).
219 Phosphorylation of the NUC polypeptide was consistently higher in NUC x 35S:SnRK1α1 than in NUC x
220 35S:SnRK1^{K48M} (significant at ZT0, 8, 16, 24 and 28). Compared to the NUC control, reporter
221 phosphorylation in NUC x 35S:SnRK1^{K48M} was significantly lower at ZT0, 8, 24 and 28 (with SnRK1^{K48M}
222 apparently functioning as a dominant negative mutant protein; Cho et al., 2016), and reporter

223 phosphorylation in NUC x 35S:SnRK1α1 was essentially control-like at ZT0, 8, 24 and 28 and
224 significantly higher at ZT16. This experiment also confirmed the rise in reporter phosphorylation in the
225 extended night, further validating the reporter.
226
227 *Diel changes in SnRK1 activity in equinoctial growth conditions*
228 The diel response of the NUC control in Supplementary Figure S3B revealed a somewhat unexpected
229 pattern, with the signal being quite high throughout the light period, decreasing rapidly at the
230 beginning of night, and then rising in the last part of the night. This was unexpected as photosynthesis
231 provides a higher C supply in the light, which is expected to inhibit SnRK1. We investigated if this
232 unexpected diel response was robust and reproducible. Independent experiment with equinoctial
233 light-dark regimes (three with NUC, two with GEN) yielded a robust and reproducible diel response
234 with SnRK1 activity at dawn being maintained during the light period, followed by a decline after
235 darkening to a minimum at about ZT16 and an increase in the last part of the night (Figure 1A). The
236 NUC and GEN lines exhibited similar responses.
237 We explored diel changes in metabolic status and in potential metabolite effectors of SnRK1
238 (Figure 1B) in the same plant material. Obvious candidates include sugars (glucose, sucrose) and starch
239 as indicators of C status, and sugar phosphates, such as Tre6P, Glc6P and Glc1P, all of which were
240 suggested previously to be directly or indirectly involved in the regulation of SnRK1 (Toroser *et al.*,
241 2000; Lu *et al.*, 2007; Zhang *et al.*, 2009; Emanuelle *et al.*, 2015; Broeckx *et al.*, 2016; Hulsmans *et al.*,
242 2016; Zhai *et al.*, 2017; 2018; Ruiz-Gayosso *et al.*, 2018). The diel responses of metabolites were
243 reproducible and resembled previous reports (Lunn *et al.*, 2006; Sulpice *et al.*, 2014; Mengin *et al.*,
244 2017; Flis *et al.*, 2019; Moraes *et al.*, 2019). In brief, starch accumulated in a near-linear manner during
245 the light period and was mobilized in a near-linear manner at night, sucrose gradually increased in the
246 light to a peak at ZT12 (ED) and gradually decreased during the night, and glucose levels showed a 1.5-
247 to 3-fold transient increase at ZT4 but otherwise remained relatively low throughout the diel cycle
248 (see also Mengin *et al.*, 2017). Tre6P changed in parallel with sucrose, as expected from previous
249 studies (Martins *et al*., 2013; Figueroa *et al*., 2016; Peixoto *et al*., 2021). Glc6P and Glc1P levels
250 remained fairly stable throughout the day, rose at the beginning of the night until ZT16 and then
251 decreased.
252 These experiments did not reveal pronounced reciprocal changes in Tre6P levels and SnRK1
253 activity during the diel cycle, except late in the night (between ZT16-24) when Tre6P levels decreased
254 and phosphorylation of both NUC and GEN polypeptides increased. In addition, no reciprocal changes
255 were observed between NUC or GEN phosphorylation and sugar levels, except for sucrose in the last
256 part of the night. However, Glc6P and Glc1P did show a reciprocal relationship with SnRK1 activity

257 through the night; Glc6P and Glc1P initially increased after dusk (from ZT12-16), and then decreased
258 (from ZT16-24), while phosphorylation of NUC and GEN decreased during the first part of the night
259 and then increased (see later for more analysis).
260
261 *Perturbations of the light regime*
262 To further explore how SnRK1 is regulated by changes in metabolites, by light and/or by endogenous
263 (e.g. circadian clock) rhythms, we next investigated NUC and GEN phosphorylation during
264 perturbations of the light regime, including standard equinoctial light treatments as a control.
265 The first treatment was based on a perturbation described in Moraes *et al.* (2019). Plants were
266 grown in equinoctial conditions under 160 µmol m^{-2} s^{-1} irradiance for 19 days, and then transferred to
267 60 µmol m^{-2} s^{-1} for one light period (treatment light period), darkened at ZT12 at the same time as in
268 the initial growth conditions (treatment night) and then returned to 160 µmol m^{-2} s^{-1} on the next day
269 (recovery light period). Control plants were left in the original growth conditions (Figure 2). The
270 response of starch and sugars closely resembled that in Moraes *et al.* (2019). Compared to control
271 plants, a single low-irradiance day led to slower starch accumulation and a decrease in the levels of
272 sucrose and glucose during the treatment light period, and slower starch mobilization and lower sugar
273 levels in the following night (Figure 2A; Supplementary Dataset S1 – Exp.3). During the recovery light
274 period, glucose was higher and starch accumulation was faster than in the light period in control
275 plants, indicating that growth was restricted (see also Gibon *et al.*, 2004; Sulpice *et al.*, 2014b; Mengin
276 *et al.*, 2017).
277 Phosphorylation of NUC and GEN polypeptides (Figure 2B) showed a combination of expected
278 and unexpected features, which were partially shared between the NUC and GEN lines but also
279 showed some differences. Rather surprisingly, a sudden decrease in irradiance had no immediate
280 impact on NUC or GEN phosphorylation in the treatment light period. However, it did have significant
281 effects in the following night and during the recovery day. For NUC, there was no initial drop in
282 phosphorylation after darkening, with the result that phosphorylation was significantly higher than
283 the control (where it decreased in the first part of the night). However, after ZT20, there was a sharp
284 decrease in NUC phosphorylation and this persisted during the recovery light period. For GEN,
285 phosphorylation increased significantly compared to the control by ZT16, and increased even further
286 as the night progressed, followed by a decrease to control levels in the recovery light period.
287 It is rather surprising that, after a shift to low light, the decrease of sugar levels was not
288 accompanied by an increase in NUC or GEN phosphorylation in the light period. This indicates that at
289 this time in the diel cycle, nuclear and extra-nuclear SnRK1 activity are not responding to current C
290 availability as reflected by overall sugar levels. At night, NUC and GEN phosphorylation were higher in

291 plants exposed to low irradiance during the preceding light period than in the control, reflecting the
292 lower C availability, but this response was much more marked for GEN than NUC. Indeed, NUC signal
293 fell at the end of the night, even though sugars remained low. In the recovery day, when sugars were
294 higher than in the control, NUC phosphorylation was lower than the control as would be expected if
295 it were responding to current C availability. However, GEN phosphorylation was high, indicating that
296 extra-nuclear SnRK1 activity was not responding to current C availability. Indeed, considering that GEN
297 is a composite of nuclear and of cytoplasmic activity, it is likely that cytoplasmic SnRK1 activity was
298 actually increased since NUC signal activity was decreased at this time (see above).

299 The second treatment was based on an experiment reported by Fernandez *et al.* (2017), in
300 which plants were grown in equinoctial conditions with 160 µmol m^{-2} s^{-1} irradiance for 19 days and
301 then transferred to continuous lower irradiance. The original study of Fernandez *et al*. (2017)
302 investigated starch degradation in the light, and the low irradiance was used to avoid over-
303 accumulation of starch in continuous light. The rationale for the current experiment was to test
304 whether the diel changes in phosphorylation activity of SnRK1 are driven by the external light regime
305 or by endogenous cues.

306 We grew plants in standard equinoctial conditions at 160 µmol m^{-2} s^{-1}, then transferred them,
307 at dawn on day 20 after sowing, to continuous light with an irradiance of 90 µmol m^{-2} s^{-1}, and sampled
308 them at 4-h intervals for 32 h (Figure 3). Control plants were left in the original growth conditions.
309 After transfer to continuous low light, starch accumulated for about 12 h, although more slowly than
310 in control plants, and starch levels then plateaued or even declined slightly in the subjective night from
311 ZT12 onwards (Figure 3A; Supplementary Dataset S1 – Exp.4). Sugar levels were lower than in the
312 control in the subjective day period (ZT0-12) but rose to reach higher levels from ZT16 onwards. These
313 changes of starch and sucrose reflect a gradual but progressive increase in the rate of starch
314 mobilization from about ZT10 onwards (see Fernandez *et al.*, 2017 for details). Compared to the
315 control, Glc6P was only marginally and non-significantly lower in the subjective day, and was
316 consistently lower in the subjective night (Supplementary Figure S4). Once again, we observed that
317 lower sugar levels during the first 12 h of the 24-h cycle were not accompanied by a significant increase
318 in phosphorylation of NUC or GEN, which essentially exhibited a control-like response until ZT12
319 (Figure 3; Supplementary Dataset S1 – Exp.4). In both lines, SnRK1 activity in continuous low light was
320 higher in the subjective night than in the control during the night. Nevertheless, the decline in SnRK1
321 activity that is observed after darkening control plants at ZT12 was also observed under low
322 continuous light, although in a weakened form. NUC phosphorylation showed a gradual significant
323 decrease (relative to ZT12) from ZT14 to ZT24, while GEN phosphorylation started to decrease by ZT12

324 and declined until ZT16 (Figure 3B). In the next subjective day, phosphorylation levels of both NUC
325 and GEN resembled those in the control.
326 These observations confirmed that a fall in C availability due to decreased irradiance does not
327 lead to increased SnRK1 activity in the first part of the 24-h cycle. They also point to an endogenous
328 component contributing to the decline in SnRK1 activity from about ZT12 onwards. Furthermore, we
329 noted a reciprocal relationship between diel changes in Glc6P and SnRK1 activity, particularly with
330 NUC phosphorylation.
331
332 *Response in a T28 cycle*
333 The Arabidopsis circadian clock is mainly entrained by light at dawn and imposes an endogenous 24-
334 h rhythmicity even when the external cycle deviates from 24 h (Millar *et al.*, 1995; Locke *et al.*, 2005;
335 Graf *et al.*, 2010). Growing plants in a light-dark cycle that deviates from 24 h is therefore a good way
336 to search for oscillatory responses that are driven directly or indirectly by the clock.
337 We grew plants in a 14-h light / 14-h dark (T28) or a standard 12-h light / 12-h dark (T24) cycle
338 for 19 days with 160 µmol m^{-2} s^{-1} irradiance and harvested them at 4-h intervals on day 20 after sowing,
339 including a 4-h or 8-h period of extended darkness for the T28 and T24 control, respectively (Figure
340 4). As previously seen (Graf *et al.*, 2010), in a T28 cycle starch is exhausted at about ZT24, resulting in
341 transient C starvation and low sucrose levels from ZT24 to ZT28 (i.e., the four hours preceding the next
342 dawn) (Figure 4A; Supplementary Dataset S1 – Exp.5) as well as lower Glc6P levels through the night
343 (Supplementary Figure S5A). Correspondingly, phosphorylation of NUC and GEN at ZT0 (dawn) was
344 almost 6- and 3-fold higher in the T28 cycle than the T24 cycle, comparable to the increase observed
345 after extending the night in a T24 cycle (Figure 4B; Supplementary Dataset S1 – Exp.5, see also
346 Supplementary Fig. S3A). After illumination, NUC and GEN phosphorylation decreased strongly in a
347 T28 cycle, falling to levels that were lower than in a T24 cycle for most of the remaining light-dark
348 cycle (significant for both NUC and GEN at ZT8, ZT14 and ZT24). Importantly, NUC and GEN
349 phosphorylation decreased between ZT12 and ZT14 in a similar manner in both the T28 and T24 cycle
350 plants, even though the former were still in the light while the latter were already in the dark. Together
351 with the response in continuous light (see above), these observations point to a component with 24-
352 h rhythmicity contributing to the regulation of SnRK1 activity.
353
354 *Manipulation of Tre6P levels*
355 Tre6P is a signal of sucrose levels (Lunn *et al.*, 2006; 2014; Figueroa and Lunn, 2016; Fichtner and Lunn,
356 2021) and is widely accepted as an inhibitor of SnRK1, at least *in vitro* (Zhang *et al.*, 2009; Zhai *et al.*,
357 2018). However, the evidence that these interactions occur *in vivo* is largely correlative (Martínez-

358 Barajas *et al.*, 2011; Wingler *et al.*, 2012; Nunes *et al.*, 2013; Henry *et al.*, 2015; Nuccio *et al.*, 2015;
359 Griffiths *et al*., 2016; Peixoto *et al.*, 2021; Zacharaki *et al*., 2022). We exploited our SnRK1 reporter
360 lines to develop a genetic approach to test whether Tre6P inhibits SnRK1 activity *in vivo*. We have
361 previously used inducible-TPS (iTPS) lines, expressing the *Escherichia coli* TPS under the control of the
362 *Aspergillus nidulans* ethanol-inducible ALCOHOL DEHYDROGENASE REGULATOR (alcR) and alcA
363 promoter to investigate the impact of a short-term induced increase in Tre6P on starch, organic acid
364 and nitrogen metabolism (Martins et al.,2013; Figueroa et al., 2016). We now introgressed the NUC
365 and GEN reporters into a well characterized iTPS line (TPS29.2; Martins et al., 2013) and into its
366 corresponding empty-vector control, alcR. Four homozygous lines were generated: two lines
367 containing both the alcR gene and the inducible *TPS* (NUC x iTPS #6.3 and GEN x iTPS #2.4), and two
368 control lines with only the alcR gene (NUC x alcR #1.2 and GEN x alcR #1.1).

369 These lines were grown in long-day conditions (16-h photoperiod, 160 µmol m^{-2} s^{-1} irradiance).
370 On day 21 after sowing, plants were sprayed at ZT1 with either water (control) or 2% (v/v) ethanol to
371 induce the expression of the bacterial TPS (Figure S6). Two whole rosettes were harvested and pooled
372 at 4, 6 and 8h after spraying. Transient expression of the bacterial TPS protein was detectable within
373 4 h of induction (Supplementary Figure S6B), consistent with previous experiments with the parental
374 iTPS line (Martins *et al.*, 2013; Figueroa *et al.*, 2016). After ethanol induction, there was a strong and
375 consistent decrease in SnRK1 nuclear activity (in NUC x iTPS) and a small decrease in overall SnRK1
376 activity after 4 and 6 but not after 10-h in GEN x iTPS (Supplementary Figure S6A; Supplementary
377 Dataset S1 – Exp.6). This led us to focus on the NUC x iTPS line (#6.3) in subsequent experiments. There
378 was no consistent effect of ethanol on NUC or GEN phosphorylation in the control alcR lines, in which
379 alcR is expressed but there is no bacterial *TPS* gene to be expressed under the control of the alcA
380 promoter. This control excludes any risk of off-target effects in the presence of ethanol or due to
381 expression of alcR (Randall, 2021).

382 To confirm the inhibitory effect of Tre6P induction in the light period, we conducted a more
383 extensive experiment. Line #6.3 was grown in equinoctial conditions under 160 µmol m^{-2} s^{-1} irradiance
384 for 20 days (the standard conditions of previous experiments), sprayed on 21 DAS with either water
385 or 2% (v/v) ethanol at ZT4, and triplicate samples were harvested at ZT7, 9 and 11 and separately
386 analysed (Figure 5; Supplementary Dataset S1 – Exp.7). Ethanol spraying led to a 41, 169 and 130%
387 increase in Tre6P levels at ZT7, ZT9 and ZT11, compared to control plants (Figure 5). Starch
388 accumulation was marginally enhanced, sucrose levels decreased at ZT7 and ZT11 (Figure 5), reducing
389 sugars were not consistently or significantly affected, and the levels of many organic acids increased
390 (Supplementary Figure S7; Supplementary Dataset S1 – Exp.7), as previously reported by Figueroa *et*
391 *al.* (2016). NUC phosphorylation showed a significant but small decrease (12-23%) following ethanol

392 spraying, compared to the water sprayed control (Figure 5). This provides evidence that Tre6P indeed
393 inhibits nuclear SnRK1 activity *in vivo*, but the impact seems to be rather small at the whole-rosette
394 level.

395 We hypothesized that if Tre6P were not the only regulator of SnRK1, other factors might
396 counteract, and thereby mask, the effect of Tre6P. Therefore, we carried out a further experiment in
397 which TPS was induced in conditions when sugars and other metabolites were low, and might not
398 mask the expected inhibition by Tre6P. Plants were grown in short-day conditions (6-h light / 18-h
399 dark) for 21 DAS with 160 µmol m^{-2} s^{-1} irradiance, sprayed with either water or 2% (v/v) ethanol
400 towards the end of the night (ZT20) and harvested at ZT20, 22, 24, 25 and 27 (Figure 6). We included
401 an alcR control line, and all comparisons were made between ethanol-induced NUC x iTPS (#6.3) and
402 ethanol-induced NUC x alcR #1.2 as the control. Under these conditions, starch was almost completely
403 exhausted and soluble sugars were at low levels (Supplementary Figure S8A). Tre6P levels declined
404 strongly between ZT20 and ZT27 in the control. Induction of TPS slowed down this decline (Figure 6),
405 with Tre6P levels at ZT24, 25 and 27 being significantly higher in ethanol-sprayed NUC x iTPS #6.3 than
406 in the NUC x alcR (#1.2) control at the same time (by 59, 112 and 33% , respectively). Phosphorylation
407 of NUC in the control rose between ZT20 and ZT24, and rose further at ZT25 and ZT27 (Figure 6). This
408 resembles the response of wild-type plants at the end of the night and in an extended night (see
409 above). Unexpectedly, induction of TPS did not attenuate but instead promoted this increase in
410 nuclear SnRK1 activity.

411 The increase in Tre6P levels was accompanied by a slight slowing of starch breakdown and
412 lower glucose levels (Supplementary Figure S8A). This confirms the response previously reported in
413 Martins *et al.* (2013), but in the present case for induction at a later time in the night. The increase in
414 Tre6P levels was also accompanied by increases in malate, pyruvate and glycerol 3-phosphate (Gly3P)
415 and a decrease in phospho*enol*pyruvate (PEP) levels (Supplementary Figure S8B; Supplementary
416 Dataset S1 – Exp.8), indicating that the stimulation by Tre6P of anaplerotic flux that was previously
417 reported in the light (Figueroa *et al*., 2016) may also occur at the end of the night. Some of these
418 downstream responses to elevated Tre6P may lead to the unexpected increase in nuclear SnRK1
419 activity after iTPS induction.

420 Overall, these results show that Tre6P is not the sole regulator of SnRK1, and its inhibitory
421 effect appears to be context dependent. Indeed, in some conditions, secondary changes caused by
422 Tre6P induction may lead, indirectly, to a stronger positive effect on SnRK1 activity than the direct
423 inhibitory effect of elevated Tre6P itself.

424

425 *Correlation analysis of relationships between SnRK1 activity and metabolite levels*

426 Taken together, our experiments point to complex and somewhat flexible regulation of SnRK1 activity
427 in conditions where C status is changing in a range above that prevailing during starvation. We
428 therefore investigated more systematically the relationship between diel changes of metabolite levels
429 and NUC or GEN phosphorylation.

430 We did this first in the five control experiments in equinoctial conditions of Figure 1. We
431 performed regression analysis separately for each experiment on all biological replicates and time
432 points across the diel cycle (Table I, for plots see Supplementary Dataset S2). Tre6P levels were not
433 correlated with either NUC (R^2 = 0.007, 0.004 and 0.004) or GEN phosphorylation (R^2 = 0.001 and
434 0.046). Glc6P levels were not consistently related to NUC phosphorylation with R^2 values of 0.048, 0.21
435 (negative and significant, P = 0.022) and 0.02 but were negatively correlated with GEN
436 phosphorylation with R^2 values of 0.22 (P = 0.03) and 0.58 (P = 2.24×10^{-5}). Similar relationships were
437 observed for Glc1P which, due to the near-equilibrium reaction catalysed by phosphoglucomutase,
438 can be expected to change in parallel with Glc6P. Starch was not correlated with either NUC or GEN
439 phosphorylation. Sucrose was not correlated with NUC and was negatively correlated with GEN
440 phosphorylation in one but not the other experiment. Glucose was not correlated with NUC, and
441 positively correlated with GEN phosphorylation in one but not the other experiment.

442 We also performed regression analysis separately on the light period (ZT4-12) and night (ZT16-
443 24) datasets (Supplementary Table S1). There were almost no significant relationships in the light
444 period. This can be expected as even though the levels of most sugars, sugar-phosphates and many
445 other metabolites change, SnRK1 activity is rather constant during the light period. During the night
446 there were many negative relationships between NUC/GEN phosphorylation and many metabolites,
447 including Tre6P, Glc6P, Glc1P, starch and sucrose. These negative relationships often reflect falling
448 levels of many metabolites towards the end of the night, as starch is gradually exhausted. They may
449 individually or collectively contribute to the rise in NUC and GEN activity at this time.

450 Pairwise correlation analyses between metabolites (Supplementary Table S2) revealed that
451 most of the measured metabolites are positively correlated with each other. This reflects the highly
452 coordinated nature of the changes in metabolism in diel cycles, and underlines that some of the
453 observed correlations between metabolites and NUC or GEN phosphorylation may be secondary.

454 The diel changes in SnRK1 activity and metabolite levels include abrupt changes after
455 illumination or darkening. These may not be well represented in correlations based on changes across
456 the entire cycle. To place more weight on such transient changes, we calculated the difference
457 between the average absolute levels at consecutive time points and divided this by the time difference
458 to obtain the direction and rate of change of a given trait in a given time interval. Compared to
459 absolute values, derivative values provide more information about changes in the balance in

460 metabolism. These derivative values were used for linear regression analyses as described above,
461 except that analyses were only performed for the entire diel cycle (Supplementary Table S3;
462 Supplementary Dataset S2). Changes in both NUC and GEN phosphorylation are significantly and
463 negatively correlated to changes in Glc6P and Glc1P, with changes in Glc6P showing the strongest
464 reciprocal agreement with changes in GEN (highest R^2 and lowest p-values).

465 We also performed correlation analyses in the experiments where plants were transferred to
466 continuous light, or grown in T28 cycles, or in which iTPS lines were used to elevate Tre6P levels
467 (Supplementary Dataset S2; Supplementary Tables S4-5, Supplementary Text S1). These analyses
468 again detected correlations between NUC or GEN phosphorylation and Glc6P and Glc1P, and also with
469 Tre6P. Further, in the experiments in which Tre6P was induced in the light period, (Fig 5), NUC
470 phosphorylation correlated negatively with Tre6P in the control plants (R^2 = 0.67, p = 0.76) but not
471 when ethanol was sprayed to increase Tre6P (R^2 = 0.12, p = 0.004) (Supplementary Table S6). This is
472 consistent with the idea that SnRK1 activity is regulated by a network including Tre6P and that this
473 network adjusts to decrease the sensitivity to Tre6P when Tre6P levels are artificially elevated.

474

475 **Discussion**

476 *Monitoring* in vivo *SnRK1 activity in plants by expression of a chimeric protein reporter*

477 Two approaches have been widely utilized to study the regulation of SnRK1 activity in plants. One is
478 *in-vitro* phosphorylation assays using a peptide with a conserved SNF1/SnRK1/AMPK recognition
479 sequence (Dale *et al.*, 1995). *In-vitro* studies are useful for identifying potential ligands and regulators,
480 including interacting proteins, and can reveal changes in maximum catalytic activity of SnRK1.
481 However, removal of the enzyme from its *in-vivo* context means that activity measurements on *in-*
482 *vitro* extracts provide only a limited information about activities *in vivo* The other approach is to
483 monitor *in vivo* readouts of SnRK1 activity, such as changes in the abundance of marker gene
484 transcripts (Baena-González *et al.*, 2007; Zhang *et al.*, 2009; Ramon *et al.*, 2019; Crepin and Rolland,
485 2019). However, while relatively easy to quantify, transcripts are only indirect readouts of SnRK1
486 activity. Their abundance reflects changes in the activity of transcriptional regulators that are the
487 direct targets for phosphorylation by SnRK1, but can also be influenced by SnRK1-independent
488 changes in transcriptional or post-transcriptional regulation. The ACC1-based polypeptide reporters
489 developed by Deroover *et al*. (2016) have been used to monitor *in-vivo* SnRK1 activities in Arabidopsis
490 (Sanagi et al., 2021; Muralidhara et al., 2021; Henninger et al., 2021; Belda-Palazon et al., 2022), and
491 we applied this approach to study *in-vivo* SnRK1 activity during the diel cycle in Arabidopsis rosettes.
492 This approach does have some potential limitations. The ACC1-based polypeptide might be
493 phosphorylated by other protein kinases in addition to SnRK1, or the extent of phosphorylation may

494 be affected by changes in the activity of endogenous protein phosphatases. Further, the approach
495 detects phosphorylation of a heterologous polypeptide, and so might not capture modifications of
496 SnRK1 function that alter its ability to recognize different endogenous protein targets. In addition to
497 the tests performed in leaf mesophyll protoplasts by Sanagi et al. (2021), we validated our approach
498 by confirming that phosphorylation of the reporter increased when SnRK1 activity *in planta* was
499 enhanced by extended darkness (Supplementary Figure S3A) or overexpression of SnRK1α1, and that
500 phosphorylation of the reporter decreased when SnRK1 activity was suppressed by expression of a
501 dominant negative form (35S:SnRK1α1^{K48M}; Supplementary Figure S3B). Nevertheless, the potential
502 complications noted above should be borne in mind when interpreting the results.
503 SnRK1 protein is located in the nucleus and in various extra-nuclear locations, and probably
504 has different targets in each of these cellular locations (see Introduction and Crozet *et al.*, 2014; Ruiz-
505 Gayosso *et al.*, 2018; Ramon *et al.*, 2019; Baena-González and Lunn, 2020). We introduced GFP-tagged
506 reporter constructs with a nuclear localization sequence (NUC) and without a nuclear localization
507 sequence (GEN), and confirmed that the former is localized to the nucleus, whereas the latter has a
508 more general location inside and outside the nucleus (Supplementary Figure S2). In many treatments,
509 including unperturbed diel cycles (Figure 1) and after transfer to extended darkness (Supplementary
510 Figure S3A), the phosphorylation state of the NUC and GEN peptides changed in a qualitatively similar
511 manner. However, in some perturbations they changed in a dissimilar or even opposite manner (see
512 Figures 2-3), presumably reflecting differing or even opposing changes in SnRK1 activity inside and
513 outside the nucleus, which might be due to differential regulation or to altered subcellular distribution
514 of SnRK1.
515
516 *Diel changes in SnRK1 activity point to it operating in a network that buffers C status*
517 It is well known that SnRK1 activity increases in stress and starvation conditions (Baena-Gonzalez *et*
518 *al.*, 2007; Baena-Gonzalez and Sheen, 2008; Mair *et al.*, 2015; Cho et al., 2016; Pedrotti *et al.*, 2018;
519 Ramon *et al.*, 2019). However, it has emerged that SnRK1 also plays a role in benign conditions (Ramon
520 *et al.*, 2019; Baena-González and Lunn, 2020; Peixoto *et al.*, 2021). After establishing that our *in vivo*
521 assay captures the expected increase in SnRK1 activity in C-depleted conditions, we focused on
522 monitoring SnRK1 activity in conditions where C availability is changing but without stressful extremes
523 of C starvation or surplus. To do this, we grew Arabidopsis in a 12-h photoperiod with 160 µmol m^{-2} s^{-}
524 ^{1} irradiance as a standard condition in which growth is restricted by the C supply, but not strongly
525 (Sulpice *et al.*, 2014).
526 One major finding was that *in-vivo* SnRK1 activity was relatively high in the light period, fell
527 after ZT12 (coinciding with darkening in our standard growth conditions) to a minimum at ZT16 and

528 then rose until the end of the night (Figure 1). Activity during the unperturbed diel cycle was several
529 times lower than in extended darkness or other treatments that led to C depletion (see Figure 4, Figure
530 6, Supplementary Fig 3A). Nevertheless, it was unexpected to observe higher SnRK1 activity in the light
531 period than during the first part of the night, because photosynthesis provides far more C in the light
532 than can be provided by mobilizing C reserves like starch in the night. Plants face a daily challenge to
533 balance the utilization of newly fixed C for immediate growth with the need to lay down C reserves
534 (e.g. starch) and to use these prudently to survive through the night. Therefore, plants must carefully
535 regulate the rate of starch accumulation in the light period, the rate of starch mobilization at night,
536 and the rate at which C is used for growth at different times in the diel cycle (Ishihara *et al.*, 2015;
537 Ivakov *et al.*, 2017; Mengin *et al.*, 2017). The diel pattern of SnRK1 activity that we observed
538 presumably reflects coordinated regulation of C utilization for reserve formation and growth
539 throughout the diel cycle. Incidentally, the relatively low SnRK1 activity during the night adds to the
540 evidence that C homeostasis is maintained across the diel light-dark cycle. In agreement, sucrose levels
541 remained relatively high for much of the night.

542 A second unexpected finding was that SnRK1 activity did not increase in response to a
543 decrease in overall C availability in the light. Illumination from dawn onwards at a lower irradiance
544 than growth irradiance did not lead to an increase in the phosphorylation status of either the NUC or
545 GEN reporter polypeptides, compared to that at growth irradiance (Figures 2 and 3). Although
546 photosynthesis was not measured in these experiments, the low irradiance treatments did lead to a
547 consistent decrease in the levels of sucrose and reducing sugars (Figures 2B and 3B; Supplementary
548 Dataset S1 – Exp.3-4; see also Moraes e*t al*., 2019). Further, these changes in irradiance occurred in
549 the range where Arabidopsis photosynthesis is light-limited (see Borghi *et al.*, 2019), and previous
550 studies have shown that similar drops in irradiance lead to a large decrease in photosynthetic rate
551 (see Fernandez *et al*., 2017; Moraes *et al*., 2019). On the other hand, treatments that led to a
552 decreased dusk starch content and slower rate of starch mobilization during the night did lead to a
553 consistent increase *in-vivo* SnRK1 activity in the first part of the night.

554 These observations point to SnRK1 being regulated in a more flexible manner in the light than
555 in the dark. This flexibility is also revealed by the response when plants are transferred to low
556 irradiance for one light period and then returned to growth irradiance. This perturbation led to higher
557 levels of sugars and faster accumulation of starch when plants were returned to growth irradiance,
558 compared to control plants that had been left at growth irradiance (Figure 2B). These observations
559 indicate that low irradiance results in a restriction of growth on the following day after returning plants
560 to previous growth irradiance (see also Moraes et al., 2019). SnRK1 activity showed a complex pattern
561 after returning to the previous growth irradiance (Figure 2); phosphorylation of NUC was lower than

562 in control plants, reflecting the higher levels of sugars, whereas phosphorylation of GEN resembled
563 that in control plants implying that extra-nuclear SnRK1 activity was higher than in control plants
564 despite sugar levels also being higher. It is known that growth in the light period is restricted when
565 Arabidopsis experiences a shortfall in C in the preceding 24-h cycle (Gibon et al., 2004; Sulpice *et al*.,
566 2014; Flis et al., 2016; Mengin *et al*., 2017; Moraes *et al*., 2019). Our observations indicate that
567 increased extranuclear SnRK1 activity might contribute to this restriction of growth and the resulting
568 increase in starch accumulation.

569 There may also be more ways for the plant to cope with a lower rate of photosynthesis in the
570 light than there are to adjust to a shortfall of starch at night. For example, the impact of decreased
571 irradiance on Glc6P levels in the light period was less marked than the impact on sugar levels
572 (Supplementary Figure S4, see also Moraes et al., 2019). This may reflect compensatory responses
573 that buffer the level of this key metabolic intermediate in the light, for example, by decreasing starch
574 synthesis, and by decreasing consumption of hexose phosphates for sucrose synthesis in the cytosol
575 by allosteric and post-transitional inhibition of sucrose-phosphate synthase (Huber and Huber, 1996;
576 Smith and Stitt, 2007; Lunn, 2016).

577 A third finding was that an endogenous circadian rhythm may contribute to the diel changes
578 in SnRK1 activity, at least in the middle of the 24-h cycle, when SnRK1 activity decreased between
579 about ZT12 and TT16. The decrease after ZT12 was partly retained in low continuous light (Figure 3)
580 and was also observed in plants growing in a T28 cycle, even though they were in the light between
581 ZT12 and ZT14 (Figure 4). The parallel changes in sugars and predicted extra-nuclear SnRK1 activity
582 after returning plants from low to growth irradiance may also point to an endogenous signal that
583 relays information about C status in the previous 24-h cycle.

584

585 *SnRK1 activity may be regulated by multiple metabolic inputs including Tre6P and hexose phosphates*

586 The unexpected diel response pointed to SnRK1 operating within a network that controls C utilization
587 in the daytime and at night to maintain C homeostasis. SnRK1 activity integrates various inputs
588 including multiple signals from metabolism (Polge and Thomas, 2007; Baena- González and Sheen,
589 2008; Wurzinger *et al.*, 2018). We asked to what extent diel changes in SnRK1 activity are accompanied
590 by reciprocal changes in the levels of sugars that might be viewed as indicators of C availability, or
591 reciprocal changes in the levels of metabolites, like Tre6P, Glc6P and Glc1P, that are known to inhibit
592 SnRK1 *in vitro* (Toroser *et al.*, 2000; Zhang *et al.*, 2009; Debast *et al.*, 2011; Delatte *et al.*, 2011; Piattoni
593 *et al.*, 2011; Nunes *et al.*, 2013a; Coello and Martínez-Barajas, 2014; Emanuelle *et al.*, 2015; Griffiths
594 *et al.*, 2016; Bledsoe *et al.*, 2017; Henry *et al.*, 2020; Baena-González and Lunn, 2020).

595 The role of Tre6P in regulation of SnRK1 has attracted wide attention (Zhang *et al.*, 2009;
596 Nunes *et al.*, 2013; Henry *et al.*, 2015; Zhang *et al.*, 2015; Bledsoe *et al.*, 2017; Baena-González and
597 Lunn, 2020). To directly test whether an induced increase in Tre6P leads to inhibition of *in-vivo* SnRK1
598 activity, we crossed our reporter constructs into lines carrying an inducible bacterial TPS construct. An
599 induced 1.4- to 2-fold increase in Tre6P in the light period indeed led to 12-23% decrease in
600 phosphorylation of the NUC reporter polypeptide (Figure 5), and a weak decrease for the GEN reporter
601 polypeptide (Supplementary Figure S6A). On the other hand, during diel cycles in wild-type plants
602 Tre6P levels did not show a consistent negative relationship to NUC or GEN phosphorylation (Figure
603 1; Table 1). Whereas Tre6P levels rose 3- to 5-fold during the light period, peaked at ZT12 (ED) and
604 then fell, (Figure 1B), SnRK1 activity did not change during the light period and, after darkening, fell
605 by 2- to 3-fold to a minimum at around ZT16 (Figure 1A). Also, comparison of the magnitude of the
606 changes in Figure 5 and Figure 1 indicates that the diel changes of Tre6P are too small to explain the
607 diel changes in NUC phosphorylation. In the last part of the night, where there was a negative
608 correlation between Tre6P levels and SnRK1 activity (Supplementary Table S1), an induced increase in
609 Tre6P resulted in an increase rather than a decrease in SnRK1 activity (Figure 6). Whilst these findings
610 provide evidence that Tre6P can contribute to the regulation of SnRK1 *in vivo*, they also show that the
611 contribution of Tre6P is context-dependent and that Tre6P is not the only or even the major factor
612 that regulates SnRK1 activity.
613 The possible role of hexose phosphates like Glc6P and Glc1P in the *in-vivo* regulation of SnRK1
614 activity has attracted less attention, despite evidence from *in-vitro* assays that they can inhibit SnRK1
615 (Toroser et al., 2000; Zhang *et al.*, 2009; Piattoni *et al.*, 2011; Nunes *et al.*, 2013). Several features of
616 our study point to them playing a role *in vivo*. First, visual inspection of diel changes under control
617 conditions reveal that Glc6P and Glc1P often change in a reciprocal manner to SnRK1 activity (Figure
618 1), peaking in the first part of the night at ZT16 at the same time as the minimum in SnRK1
619 phosphorylation activity. A negative relationship between SnRK1 and Glc6P was also observed when
620 plants were exposed to a sudden low-light day (Figure 2; see also Moraes *et al.*, 2019) or transferred
621 to continuous low light (Figure 3; Supplementary Figure S4). Second, there was a significant negative
622 correlation between Glc6P or Glc1P levels and NUC or GEN phosphorylation in some, though not all,
623 full diel cycles (Table 1) and highly consistent negative correlations in the night (Supplementary Table
624 S1). This conclusion was supported by comparison of the rates of change of Glc6P or Glc1P levels and
625 SnRK1 activity at different times in the diel cycle (Supplementary Table S3). Glc6P and Glc1P are linked
626 by the near-equilibrium reaction catalysed by phosphoglucomutase, with both changing in parallel
627 and Glc6P being about 10-fold higher than Glc1P, therefore, the observed negative relationship
628 between SnRK1 and Glc1P might be secondary to the relationship with Glc6P.

629 The question also arises what endogenous factor might be responsible for the decline in SnRK1
630 activity between ZT12 and ZT16, which occurred even when plants were not darkened at ZT12 (see
631 above). One possible explanation is that this decline is driven by diel changes in starch turnover. As
632 shown in Fernandez *et al*. (2017) and Ishihara *et al.* (2022), starch mobilization occurs simultaneously
633 with starch synthesis in the light and speeds up with time in the light, leading from about ZT10
634 onwards to a marked rise in sucrose and related metabolites, including Tre6P. This might contribute
635 to the decline in SnRK1 activity after ZT12 in continuous light. As suggested in Fernandez *et al*. (2017)
636 and Ishihara *et al*. (2022), this gradual rise in the rate of starch mobilization is itself under circadian
637 control. However, it would be premature to exclude the possibility that the circadian clock exerts a
638 more direct influence on SnRK1 activity, mirroring the recent discovery that SnRK1 is involved in
639 transcriptional regulation of the circadian clock (Jeong *et al.*, 2015; Sánchez-villarreal *et al.*, 2018; Shin
640 *et al.*, 2017; Frank *et al.*, 2018). A possible link between starch mobilization and SnRK1 activity is also
641 of interest in view of the report that the dark-expressed SnRK1β3 subunit binds maltose, pointing to
642 a possible role in regulating starch degradation or of starch degradation, via maltose, regulating SnRK1
643 activity (Ruiz-Gayosso *et al.*, 2018).
644 Taken together, our results point to both Tre6P and hexose phosphates contributing to the
645 regulation of SnRK1 *in vivo*. These metabolites provide complementary information about C status.
646 Tre6P provides information about the amount of sucrose (Lunn *et al.*, 2006; Figueroa *et al.*, 2016;
647 Figueroa and Lunn, 2016; Fichtner *et al.*, 2017; Fichtner and Lunn, 2021), which is a key long-distance
648 transport metabolite and often a C-storage molecule (Lunn, 2016). Hexose phosphate levels reflect
649 the balance between several central metabolic pathways, for example, between photosynthetic C
650 fixation and sucrose and starch synthesis in the light, and between starch mobilization, respiration
651 and biosynthesis in the dark. Further, Tre6P and hexose phosphates may have differing subcellular
652 and intercellular compartmentation. TPS1 protein, and by implication Tre6P, is partly localized to the
653 nucleus (Fichtner *et al.*, 2020) whereas hexose phosphates are likely to have a more general
654 subcellular distribution with high levels in the cytosol (Stitt *et al.*, 1980; Gerhardt *et al.*, 1987). Such
655 differences in metabolite compartmentation might underlie some of the differing responses of the
656 NUC and GEN reporters. Further, TPS1, and by implication Tre6P, is very abundant in companion cells
657 and surrounding phloem parenchyma (Fichtner *et al.*, 2020) whereas hexose phosphates are probably
658 distributed more generally across cell types, including high levels in photosynthetic mesophyll cells.
659 This may introduce important nuances into regulation of SnRK1 activity, whose detection would
660 require cell-specific expression of the reporter constructs.
661
662 *Changes in complex composition might impact on diel SnRK1 activity*

663 An additional regulatory mechanism that might contribute to observed diel changes in SnRK1 activity
664 would be changes in subunit composition, including expression or stability of its subunits, such as by
665 SUMOylation and ubiquitination of SnRK1α1, SnRK1β1, SnRK1β2 SnRK1β3, and by myristoylation of
666 SnRK1β1 and SnRK1β2 (Ruiz-Gayosso *et al.*, 2018; Ramon *et al.*, 2019; Blanco *et al.*, 2019; Wang et al.,
667 2020). These were shown to affect cellular localization, primarily by translocating SnRK1 in and out of
668 the nucleus. We cannot yet be certain whether changes in SnRK1 composition contribute to the diel
669 changes in SnRK1 activity detected using the ACC reporter constructs. In the future it would be of
670 interest to compare changes in SnRK1 composition and SnRK1 location with the relative rates of NUC
671 and GEN phosphorylation.
672
673 *Comparison of* in-vivo *SnRK1 activity with responses of SnRK1 downstream targets highlights potential*
674 *flexibility in downstream signalling pathways*
675 As already mentioned, downstream target genes identified in protoplast overexpression studies have
676 been widely used to make inferences about SnRK1 activity *in vivo*. We inspected published data to
677 learn if the diel changes in transcript abundance of these genes is consistent with the diel changes of
678 *in-vivo* SnRK1 activity, as monitored by reporter peptide phosphorylation. To do this, we focused on
679 studies in which Arabidopsis was grown in the same conditions as those used in the current study. As
680 shown in Supplementary Figure S9A, which replots data from Usadel *et al.* (2008), there was a fairly
681 consistent pattern with the abundance of SnRK1-induced transcripts falling in the light period and
682 rising during the night, and the abundance of SnRK1-repressed transcripts rising in the light and falling
683 during the night (two exceptions were *AXP* and *EXP10*). This pattern contrasts with the response of
684 the NUC/GEN reporter polypeptide phosphorylation, which was relatively high in the light period and
685 fell in the first part of the night (Figure 1A). In a second comparison, we inspected the response of a
686 set of SnRK1 target transcripts after a sudden decrease in irradiance (Moraes *et al*., 2019), similar to
687 the treatment in Figure 2 and the first 12 h after transfer to continuous low light in Figure 3
688 (Supplementary Figure S9B). Transfer from 160 to 60 µmol m^{-2} s^{-1} led, for SnRK1-induced genes, to a
689 small but consistent increase in *DIN6* and *BCAT2* and a large increase in *DIN1* transcript abundance
690 and, for SnRK1-repressed genes, to a small but consistent decrease in *CPN60α* and *Asp.P* transcript
691 abundance. This contrasts with NUC/GEN reporter polypeptide phosphorylation, which did not change
692 after transfer to low irradiance (Figures 2-3). In a recent study, Peixoto *et al*. (2021) reported that
693 abundance of SnRK1-induced transcripts was maximal at the end of the night when Tre6P levels were
694 lowest, and minimal at the end of the day when Tre6P levels peaked. However, even though the
695 changes of Tre6P levels in Peixoto *et al*. (2021) resembled those in the current study, the responses of
696 transcript abundance did not match the changes in NUC/GEN reporter polypeptide phosphorylation

697 reported in the current study. Furthermore, whilst transient elevation of Tre6P in an inducible
698 bacterial TPS line led to decreased abundance of transcripts for three SnRK1-induced genes (*BGAL,*
699 *DIN10, PYL5*) (Peixoto *et al*., 2021), consistent with involvement of Tre6P in diel regulation of SnRK1
700 signalling, it did not decrease transcript abundance for many other SnRK1-induced genes, such as
701 *DIN1*, *DIN6*, *AXP* and *EXP10*.

702 There are various possible explanations for discrepancies between SnRK1 activity as
703 monitored by phosphorylation of the NUC/GEN reporter polypeptides and SnRK1 activity as inferred
704 from the abundance of downstream transcripts. It is possible that in some cases gene expression is
705 driven by a fraction of the total SnRK1 pool, and that this fraction may remain undetectable when
706 assaying total SnRK1 activities (Baena-González and Lunn, 2020). The discrepancy may also reflect
707 multiple levels of regulation, for example, not only via changes in SnRK1 activity itself but also via
708 inputs that modify the affinity of SnRK1 for different immediate downstream targets or via inputs that
709 potentiate or attenuate different downstream signalling pathways. Such modifying factors might also
710 explain the varying responses of different SnRK1 downstream transcripts within a given experiment
711 (see above, also Griffiths *et al*., 2016), as well as between different studies. Indeed, of the top SnRK1
712 target genes, only a few changed in a reproducible manner following SnRK1 induction in protoplasts
713 versus whole plants (Baena-González *et al.*, 2007; Ramon *et al.*, 2019; Peixoto *et al.*, 2021). For
714 example, *DIN1*, *DIN6* and *CAT1*, whose expression is commonly used as a readout of SnRK1 activity,
715 are strongly upregulated in response to transient expression of SnRK1α1 in protoplasts (Baena-
716 González *et al.*, 2007), but remain unaffected in response to constitutive overexpression of SnRK1α1
717 in whole plants (Peixoto *et al.*, 2021).

718 Functionally, operation of SnRK1 in a benign diel cycle as well as during starvation mirrors the
719 differing responses of two sub-sets of C-regulated genes. Many of these show large changes in
720 expression during a regular equinoctial diel cycle (Smith and Stitt, 2007; Usadel *et al*., 2008; Cookson
721 *et al*., 2016, Flis et al., 2016). These genes may contribute to modifications of metabolism and slowing
722 down of growth, and serve to maintain C homeostasis and avoid transient periods of C starvation and
723 the resulting wasteful alternation between growth and catabolism (Ishihara et al., 2015, 2017). Other
724 C-regulated genes do not show changes in expression until starch is exhausted, and may serve to
725 orchestrate catabolic responses in conditions when the plant can no longer avoid C starvation.

726 In conclusion, by employing an *in-vivo* reporter polypeptide assay we have uncovered
727 unexpected changes in SnRK1 activity under benign light-dark cycles. Continued SnRK1 activity in the
728 light period may contribute to maintenance of diel sugar homeostasis, by restricting C utilization for
729 growth and supporting build-up of C reserves. Further, whilst demonstrating that Tre6P can inhibit

730 SnRK1 activity *in vivo*, we also show that its contribution is context dependent and that hexose
731 phosphates, and probably also other factors, interact to regulate SnRK1 activity and signalling.
732
733 **Materials and Methods**
734
735 *Plant material*
736 All Arabidopsis (*Arabidopsis thaliana* [L.] Heynh.) genotypes were in the Columbia-0 (Col-0)
737 background. Lines expressing the NUC or GEN SnRK1 reporters were generated as described in Sanagi
738 *et al.* (2021). The reporters comprise a 57-amino acid peptide derived from rat (*Rattus norvegicus*)
739 acetyl CoA carboxylase (rACC1), containing the AMPK recognition motif and Ser79 phosphorylation
740 site, fused at the C-terminus to eGFP and a double haemagglutinin tag (Supplementary Figure S1;
741 Deroover *et al.*, 2016). The NUC reporter includes an N-terminal SV40 nuclear localization signal that
742 targets the reporter specifically to the nucleus, while the GEN reporter has no added nuclear
743 localization signal and is localized in both the nucleus and cytoplasm (Supplementary Figure S2). The
744 Arabidopsis (Col-0) ethanol-inducible TPS-overexpressor (iTPS 29.2) and empty-vector control AlcR
745 lines were the same as those described in Martins *et al.*, 2013. The Arabidopsis (Col-0) 35S:SnRK1α1
746 over-expression line (Jossier *et al.*, 2009) and the 35S:SnRK1α1^{K48M} line, expressing the SnRK1α1
747 subunit with a mutation that disrupts ATP binding (Cho *et al.*, 2016), were kindly provided by Elena
748 Baena-González (Instituto Gulbenkian de Ciência, Oeiras, Portugal) and Hsing-Yi Cho (National Chung-
749 Hsing University, Academia Sinica, Taiwan), respectively.
750
751 *Introgression of NUC and GEN SnRK1 reporters*
752 The NUC and GEN SnRK1 reporters were introgressed into established lines with altered SnRK1 activity
753 or inducible expression of TPS by crossing. The respective homozygous parental lines were grown in
754 soil for 4-5 weeks (see below). Pollen from the parental parent was transferred by rubbing anthers
755 from mature flowers against exposed stigmas of emasculated maternal plants under a binocular
756 microscope, and the inflorescence meristems and unopened flower buds were removed. After
757 crossing, the maternal plants were grown on, with regular watering, for 2-3 weeks until siliques had
758 fully developed and started to dry. Siliques were collected, left to dry for a further 3-4 days at room
759 temperature and then kept at 10 °C until seeds were germinated on selective media. After surface
760 sterilization by treatment with 2% (w/v) sodium hypochlorite for 5 min at room temperature and
761 washing in five changes of water, seeds were placed on 0.5x Murashige and Skoog medium (Murashige
762 and Skoog, 1962) containing 1% (w/v) sucrose and appropriate antibiotics for selection of the
763 respective transgenes from each parent: NUC/GEN phosphinothricin (Basta); 35S:SnRK1α1,

764 kanamycin; 35S: SnRK1α1^{K48M}, hygromycin; iTPS/alcR; kanamycin. The seeds were stratified for 2 days
765 at 4°C in the dark and then transferred to 22°C in continuous light at 100 µmol m^{-2} s^{-1}. After 7 days,
766 surviving seedlings were transferred to soil. The F1 plants were selfed and F2 progeny were screened
767 on selective media, as above, to identify lines that exhibit the expected susceptible: resistant ratio of
768 7:9. Individual F2 plants were selfed and the F3 progeny were screened on selective media, as above,
769 to identify lines that were homozygous for both transgenic loci.
770
771 *Plant growth and harvest*
772 Seeds were sown on a 1:1 mixture of compost (Stender AG, Schermbeck, Germany;
773 https://www.stender.de) and vermiculite in 6-cm diameter pots, covered and kept at 4°C in the dark
774 for 48 h then transferred to a controlled environment chamber (Percival E-36 L chamber, CLF Plant
775 Climatics GmbH, Weringen, Germany; https://www.plantclimatics.de/) with a 16-h photoperiod (160
776 µmol m^{-2} s^{-1} irradiance provided by white LEDs) and day/night temperatures of 21°C/19°C. After
777 germination, seedlings were transferred to 10-cm diameter pots (four or five seedlings per pot), and
778 grown as above or as described for individual experiments. Whole rosettes were harvested *in situ* and
779 immediately quenched in liquid nitrogen, with four or five plants from the same pot being pooled for
780 each biological replicate. Frozen plant material was ground to a fine powder and stored at -80°C until
781 use.
782
783 *Metabolite extraction and analysis*
784 Soluble sugars and starch were extracted and assayed enzymatically as described in Gibon *et al.* (2002)
785 with three-four biological replicates per sample type. For each biological replicate, values were
786 calculated as the average of two measurements. Tre6P, other phosphorylated intermediates and
787 organic acids were extracted with chloroform-methanol and quantified by anion-exchange high-
788 performance liquid chromatography coupled to tandem mass spectrometry as described in Lunn *et al.*
789 (2006), with modifications as described in Figueroa *et al*. (2016).
790
791 *Ethanol-inducible iTPS experiments*
792 After introgression of the NUC/GEN SnRK1 reporters, ethanol-inducible TPS (iTPS) and control alcR
793 lines (Martins *et al.*, 2013) were grown as described above. On the day of harvest, plants were sprayed
794 with either water (mock induction control) or with 2% (v/v) ethanol to induce expression of the
795 bacterial TPS and thereby increase Tre6P levels. Samples were collected and harvested as described
796 above.
797

798 *SDS-PAGE and immunoblot assay of SnRK1 reporter phosphorylation*

799 Proteins were extracted from aliquots (10 mg FW) of frozen, finely powdered plant material by
800 suspension in 100 µl of pre-warmed (90°C) sample buffer (66 mM Tris-HCl, pH 6.8, 10% (v/v) glycerol,
801 2% (w/v) sodium dodecyl sulphate, 0.13% (w/v) bromophenol blue) quickly vortex mixed, incubated
802 at 90°C for 5 min, then chilled on ice and centrifuged at 13,500 x *g* (4°C) for 3 min. Aliquots of the
803 supernatant containing approx. 12 µg of soluble protein were electrophoresed on a 12% (w/v)
804 polyacrylamide-SDS gel. Proteins were electro-blotted onto nitrocellulose membrane, visualized by
805 staining with 0.2% (w/v) Ponceau Red in 1% (v/v) acetic acid and imaged for use as a protein-loading
806 reference. After blocking in Tris-buffered saline containing 5% (w/v) milk powder, the membrane was
807 incubated overnight at 4°C with rabbit anti-phospho-acetyl CoA carboxylase (Ser79) antibody (#3661;
808 Cell Signaling Technology Europe BV, Leiden, The Netherlands; https://www.cellsignal.de) at a dilution
809 of 1:1500. After washing, NUC/GEN phosphorylation was detected by incubation with IRDye 800CW
810 goat anti-rabbit IgG (H+L) secondary antibody (Li-COR Biosciences GmbH, Bad Homburg, Germany;
811 www.licor.com) at a dilution of 1:9000 and scanning with an Odyssey Imaging Scanner (Li-COR), and
812 quantified using Image Studio Live 5.2 software (Li-COR). Total NUC/GEN polypeptide abundance was
813 detected by probing duplicate blots with a mouse anti-GFP antibody (#11814460001; Sigma Aldrich
814 (Roche), Darmstadt, Germany; www.sigmaaldrich.com) at a dilution of 1:1500, followed by incubation
815 with IRDye 680RD goat anti-mouse IgG (H+L) secondary antibody (Li-COR) at a dilution of 1:9000, and
816 quantified as above.

817 To minimize the impact of gel-to-gel variation, aliquots from an extended night sample were
818 loaded onto each gel and the signal from this sample was used to normalize the signals from the other
819 samples on the corresponding immunoblot. Two aliquots of the protein extract from each biological
820 replicate were analyzed on separate gels and, after normalization as described above, the average of
821 the two technical replicates was calculated as the reported value for that biological replicate. The
822 signal ratio pACC/GFP was used to normalize for any differences in reporter protein abundance in the
823 tissue and differences in gel loading. See Supplementary Figure S1 for further details.

824

825 *Confocal microscopy*

826 To determine the subcellular localization of the NUC/GEN SnRK1 reporter proteins, GFP was visualized
827 by laser confocal microscopy of 6-day-old seedlings. Imaging was performed on a Leica TCS SP5
828 microscope (Leica Microsystems, Wetzlar, Germany; https://www.leica-microsystems.com) using a
829 20x objective. To visualize nuclei, NUC samples were stained with 10 µg/ml propidium iodide (PI)
830 solution for 5 to 10 min. A 488 nm laser was used to excite GFP and 561 nm laser to excite PI and their

831 fluorescence emission was detected in the 524-555 nm and 571-640 nm ranges, respectively. Confocal
832 Z sections were acquired every 0.5 µm.
833
834 *Statistical analysis*
835 Technical replicates were always averaged to generate a single value for each biological replicate,
836 statistical analysis was restricted to biological replicates and performed using Sigma-Plot 14.5
837 software (Systat Software GmbH, Düsseldorf, Germany; http://www.systat.de). Significance of
838 changes in metabolite and SnRK1 activity was tested by one-way ANOVA using a pairwise multiple
839 comparison procedure, with post-hoc testing by the Holm-Sidak method ($p<0.05$), as described in each
840 figure legend.
841

842 **Acknowledgements**
843 We thank Sofie Deroover and Tom Broeckx for help with generation and selection of the NUC and GEN
844 SnRK1 reporter lines and Arun Sampathkumar for help with laser confocal microscopy.
845

846 **Funding**
847 This work was supported by the Max Planck Society (O.A., T.A.M., V.M., R.F., M.S., and J.E.L.) and by
848 KU Leuven (F.R.).
849
850 **Author contributions**: O.A. performed all experiments, statistically analysed data, and contributed to
851 paper writing; T.A.M contributed to experimental design, harvesting, measurement of metabolites
852 and data analysis. V.M. contributed to harvesting and measurement of metabolites, R.F. performed
853 LC-MS/MS metabolite analysis; F.R. conceived and generated the SnRK1 reporter constructs, M.S.
854 assisted data analysis and contributed to writing the paper. J.E.L. conceived the project, assisted data
855 analysis, and contributed to writing the paper.
856

857 **Supplementary Data**

858 **Supplementary Figure S1:** *In vivo* SnRK1 activity assay

859 **Supplementary Figure S2:** Localization of reporter peptides by confocal microscopy

860 **Supplementary Figure S3:** Validation of the NUC and GEN constructs in whole Arabidopsis rosettes

861 **Supplementary Figure S4:** Comparison of different low light treatments (supplementary to Figure 2
862 and 3)

863 **Supplementary Figure S5:** T28 and T24 cycles; diel Glc6P levels and comparison of SnRK1 activity
864 excluding time points affected by C starvation (supplementary to Figure 4).

865 **Supplementary Figure S6:** Response of NUC and GEN phosphorylation in crosses with a line containing
866 inducible bacterial TPS.

867 **Supplementary Figure S7:** Impact of transiently elevated Tre6P in the light period on the levels of
868 selected metabolites (supplementary to Figure 5).

869 **Supplementary Figure S8:** Transient elevation of Tre6P at the end of the night slows down starch
870 mobilization and leads to low glucose and high organic acid levels (supplementary to Figure 6)

871 **Supplementary Figure S9:** Transcript abundance for SnRK1 target genes during a diel cycle, after an
872 extension of the night and after a sudden decrease in light intensity for one day.

873 **Supplementary Table S1:** Correlations between metabolite levels and NUC or GEN phosphorylation,
874 performed separately for the light period and the night (supplementary to Table 1 and Figure 1).

875 **Supplementary Table S2:** Correlations between metabolite levels (supplementary to Table 1 and
876 Figure 1)

877 **Supplementary Table S3:** Correlations between changes in metabolite levels and changes in NUC or
878 GEN phosphorylation (supplementary to Table 1 and Figure 1).

879 **Supplementary Table S4:** Correlations between metabolite levels and NUC or GEN phosphorylation in
880 growth regimes that differed from the equinoctial T24 cycle (supplementary to Figures 3 and 4).

881 **Supplementary Table S5**: Summary of correlation analysis between changes in SnRK1 NUC and GEN
882 activity to changes in metabolite levels (supplementary to Figures 3 and 4).

883 **Supplementary Table S6**: Correlation analysis between metabolite levels and NUC phosphorylation
884 following transient elevation of Tre6P in the light period (supplementary to Figure 5, Supplementary
885 Dataset S2 Exp.7).

886 **Supplementary Text S1:** Correlations between in vivo SnRK1 activity and metabolites in continuous
887 light, in T28 cycles and in experiments where TPS is induced (supplementary to Supplementary Tables
888 S4-S6)

889 **Supplementary Dataset S1:** *In-vivo* SnRK1 activity and metabolite levels.

890 **Supplementary Dataset S2:** Regressions between *in-vivo* SnRK1 activity and metabolite levels.

891 **References**

892

893 **Ávila-Castañeda A, Gutiérrez-Granados N, Ruiz-Gayosso A, Sosa-Peinado A, Martínez-Barajas E,**
894 **Coello P** (2014) Structural and functional basis for starch binding in the SnRK1 subunits AKINβ2
895 and AKINβγ. Front Plant Sci **5:** 199

896 **Baena-González E, Rolland F, Thevelein JM, Sheen J** (2007) A central integrator of transcription
897 networks in plant stress and energy signalling. Nature **448**: 938–942

898 **Baena-González E, Lunn JE** (2020) SnRK1 and trehalose 6-phosphate – two ancient pathways converge
899 to regulate plant metabolism and growth. Curr Opin Plant Biol **55**: 52–59

900 **Belda-Palazón, B., Costa, M., Beeckman, T., Rolland, F., Baena-González, E.** (2022) ABA represses TOR
901 and root meristem activity through nuclear exit of the SnRK1 kinase. Proc Natl Acad Sci USA **119:**
902 2204862119.

903 **Blanco NE, Liebsch D, Díaz MG, Strand Å, Whelan J** (2019) Dual and dynamic intracellular localization
904 of Arabidopsis thaliana SnRK1.1. J Exp Bot **70**: 2325–2338

905 **Bledsoe SW, Henry C, Griffiths CA, Paul MJ, Feil R, Lunn JE, Stitt M, Lagrimini LM** (2017) The role of
906 Tre6P and SnRK1 in maize early kernel development and events leading to stress-induced kernel
907 abortion. BMC Plant Biol **17**: 1–17

908 **Borghi GL, Moraes TA, Günther M, Feil R, Mengin V, Lunn JE, Stitt M, Arrivault S** (2019) Relationship
909 between irradiance and levels of Calvin–Benson cycle and other intermediates in the model
910 eudicot Arabidopsis and the model monocot rice. J Exp Bot **70:** 5809–5825

911 **Broeckx T, Hulsmans S, Rolland F** (2016) The plant energy sensor: evolutionary conservation and
912 divergence of SnRK1 structure, regulation, and function. J Exp Bot **67**, 6215–6252

913 **Cabib E, Leloir LF** (1958) The biosynthesis of trehalose phosphate. J Biol Chem **231:** 259-75

914 **Cho H, Wen T, Wang Y, Shih M** (2016) Quantitative phosphoproteomics of protein kinase SnRK1
915 regulated protein phosphorylation in Arabidopsis under submergence. J Exp Bot **67**: 2745–2760

916 **Clough SJ, Bent AF** (1998) Floral dip: a simplified method for Agrobacterium-mediated transformation
917 of *Arabidopsis thaliana*. Plant J **16**: 735–743

918 **Coello P, Martínez-Barajas E** (2014) The activity of SnRK1 is increased in *Phaseolus vulgaris* seeds in
919 response to a reduced nutrient supply. Front Plant Sci **5**: 1–7

920 **Cookson S, Yadav UP, Klie S, Morcuende RM, Usadel B, Lunn JE, Stitt M** (2016) Temporal kinetics of
921 the transcriptional response to carbon depletion and sucrose readdition in Arabidopsis seedlings.
922 Plant Cell Environ **39:** 768-786

923 **Crepin N, Rolland F** (2019a) SnRK1 activation , signaling , and networking for energy homeostasis.
924 Curr Opin Plant Biol **51:** 29–36

925 **Crozet P, Margalha L, Confraria A, Rodrigues A, Martinho C, Adamo M, Elias CA, Baena-González E**
926 (2014) Mechanisms of regulation of SNF1/AMPK/SnRK1 protein kinases. Front Plant Sci **5:** 190
927 **Dale S, Wilson WA, Edelman AM, Hardie DG** (1995) Similar substrate recognition motifs for
928 mammalian AMP-activated protein kinase, higher plant HMG-CoA reductase kinase-A, yeast
929 SNF1, and mammalian calmodulin-dependent protein kinase I. FEBS Lett **361**: 191–195
930 **Debast S, Nunes-Nesi A, Hajirezaei MR, Hofmann J, Sonnewald U, Fernie AR, Börnke F** (2011) Altering
931 trehalose-6-phosphate content in transgenic potato tubers affects tuber growth and alters
932 responsiveness to hormones during sprouting. Plant Physiol **156:** 1754-1771
933 **Delatte TL, Sedijani P, Kondou Y, et al.** (2011) Growth arrest by trehalose-6-phosphate : an
934 astonishing case of primary metabolite control over growth by way of the SnRK1 signaling
935 pathway. Plant Physiol **157**: 160–174
936 **Delorge I, Figueroa CM, Feil R, Lunn JE, van Dijck P** (2015) Trehalose-6-phosphate synthase 1 is not
937 the only active TPS in *Arabidopsis thaliana*. Biochem J **290:** 283–290
938 **Deroover S, Ghillebert R, Broeckx T, Winderickx J, Rolland F** (2016) Trehalose-6-phosphate synthesis
939 controls yeast gluconeogenesis downstream and independent of SNF1. FEMS Yeast Res **16:**36
940 **Emanuelle S, Hossain MI, Moller IE, et al.** (2015) SnRK1 from *Arabidopsis thaliana* is an atypical AMPK.
941 Plant J **82**: 183–192
942 **Fernandez O, Ishihara H, George GM, et al.** (2017) Leaf starch turnover occurs in long days and in
943 falling light at the end of the day. Plant Physiol **174**: 2199–2212
944 **Fichtner F, Barbier FF, Feil R, Watanabe M, Annunziata MG, Stitt M, Beveridge CA, Lunn JE** (2017)
945 Trehalose 6-phosphate is involved in triggering axillary bud outgrowth in garden pea (*Pisum*
946 *sativum* L .). Plant J **92:** 611–623
947 **Fichtner F, Olas JJ, Feil R, Watanabe M, Krause U, Hoefgen R, Stitt M, Lunn JE** (2020) Functional
948 features of TREHALOSE-6-PHOSPHATE SYNTHASE1, an essential enzyme in Arabidopsis. Plant Cell
949 **32**: 1949–1972
950 **Fichtner F, Lunn JE** (2021) The Role of trehalose 6-phosphate (Tre6P) in plant metabolism and
951 development. Annu Rev Plant Biol **72:** 737-760
952 **Figueroa CM, Feil R, Ishihara H, et al.** (2016) Trehalose 6-phosphate coordinates organic and amino
953 acid metabolism with carbon availability. Plant J **85**: 410–423
954 **Figueroa CM, Lunn JE** (2016) A tale of two sugars: trehalose 6-phosphate and sucrose. Plant Physiol
955 **172**: 7–27
956 **Flis A, Sulpice R, Abel C, Ivakov A, Liput M, Millar AJ, Stitt M** (2016) Photoperiod-dependent changes
957 in the phase of core clock transcripts, and in global transcriptional outputs at dusk and dawn in
958 Arabidopsis. Plant Cell Environ **39**: 1955-1981

959 **Flis A, Mengin V, Ivakov AA, et al.** (2019) Multiple circadian clock outputs regulate diel turnover of
960 carbon and nitrogen reserves. Plant Cell Environ **42**: 549–573
961 **Frank A, Matiolli CC, Viana AJC, et al.** (2018) Circadian entrainment in arabidopsis by the sugar-
962 responsive transcription factor bZIP63. Curr Biol **28:** 2597-2606
963 **García-Salcedo R, Lubitz T, Beltran G, et al.** (2014) Glucose de-repression by yeast AMP-activated
964 protein kinase SNF1 is controlled via at least two independent steps. FEBS J **281**: 1901–1917
965 **Gerhardt R, Stitt M, Heldt HW** (1987) Subcellular metabolite levels in spinach leaves : regulation of
966 sucrose synthesis during diurnal alterations in photosynthetic partitioning. Plant Physiol **83**: 399-
967 407
968 **Gibon Y, Vigeolas H, Tiessen A, Geigenberger P, Stitt M** (2002) Sensitive and high throughput
969 metabolite assays for inorganic pyrophosphate, ADPGlc, nucleotide phosphates, and glycolytic
970 intermediates based on a novel enzymic cycling system. Plant J **30**: 221–235
971 **Gibon Y, Bläsing OE, Palacios-Rojas N, Pankovic D, Hendriks JHM, Fisahn J, Höhne M, Günther M,**
972 **Stitt M** (2004) Adjustment of diurnal starch turnover to short days: depletion of sugar during the
973 night leads to a temporary inhibition of carbohydrate utilization, accumulation of sugars and
974 post-translational activation of ADP-glucose pyrophosphorylase in the following light period.
975 Plant J **39**: 847–862
976 **Glab N, Oury C, Guérinier T, Domenichini S, Crozet P, Thomas M, Vidal J, Hodges M** (2017) The impact
977 of *Arabidopsis thaliana* SNF1-related-kinase 1 (SnRK1)-activating kinase 1 (SnAK1) and SnAK2 on
978 SnRK1 phosphorylation status: characterization of a SnAK double mutant. Plant J **89:** 1031–1041
979 **Glinski M, Weckwerth W** (2005) Differential multisite phosphorylation of the trehalose-6-phosphate
980 synthase gene family in *Arabidopsis thaliana*: a mass spectrometry-based process for
981 multiparallel peptide library phosphorylation analysis. Mol Cell Proteomics **4**: 1614-1625
982 **Goddijn OJM, van Dun K** (1999) Trehalose metabolism in plants. Trends Plant Sci **4:** 315–319
983 **Graf A, Schlereth A, Stitt M, Smith AM** (2010) Circadian control of carbohydrate availability for growth
984 in Arabidopsis plants at night. Proc Natl Acad Sci USA **107**: 9458–9463
985 **Griffiths CA, Sagar R, Geng Y, et al.** (2016) Chemical intervention in plant sugar signalling increases
986 yield and resilience. Nature **540**: 574–578
987 **Hara LEO, Paul MJm Wingler A** (2013) How do sugars regulate plant growth and development? New
988 insight into the role of trehalose-6-phosphate. Mol Plant **6**, 261–274
989 **Hardie DG, Carling D** (1997) The AMP-activated protein kinase – fuel gauge of the mammalian cell?
990 Eur J Biochem **246**: 259–273
991 **Hardie DG, Carling D, Carlson M** (1998) The AMP-activated/SNF1 protein kinase subfamily: metabolic
992 sensors of the eukaryotic cell? Annu Rev Biochem **67**: 821–855

993 **Harthill JE, Meek SEM, Morrice N, Peggie MW, Borch J, Wong BHC, Mackintosh C** (2006)
994 Phosphorylation and 14-3-3 binding of Arabidopsis trehalose-phosphate synthase 5 in response
995 to 2-deoxyglucose. Plant J **47:** 211–223
996 **Henninger M, Pedrotti L, Krischke M, Draken J, Wildenhain T, Fekete A, Rolland F, Müller MJ,**
997 **Fröschel C, Weiste C, Dröge-Laser W** (2022) The evolutionarily conserved kinase SnRK1
998 orchestrates resource mobilization during Arabidopsis seedling establishment. Plant Cell **34**: 616-
999 632
1000 **Henry C, Bledsoe SW, Griffiths CA, Kollman A, Paul MJ, Sakr S, Lagrimini LM** (2015) Differential role
1001 for trehalose metabolism in salt-stressed maize. Plant Physiol **169**: 1072–1089
1002 **Henry C, Watson-Lazowski A, Oszvald M, Griffiths C, Paul MJ, Furbank RT, Ghannoum O** (2020) Sugar
1003 sensing responses to low and high light in leaves of the C_4 model grass *Setaria viridis*. J Exp Bot
1004 **71**: 1039–1052
1005 **Herzig S, Shaw RJ** (2017) AMPK: guardian of metabolism and mitochondrial homeostasis. Nat Rev Mol
1006 Cell Biol **19:** 121-135
1007 **Huber SC, Huber JL** (1996) Role and regulation of sucrose-phosphate synthase in higher plants. Annu
1008 Rev Plant Physiol Plant Mol Biol **47**: 431–444
1009 **Hulsmans S, Rodriguez M, de Coninck B, Rolland F** (2016) The SnRK1 energy sensor in plant biotic
1010 interactions. Trends Plant Sci **21**: 648–661
1011 **Hwang G, Kim S, Cho J-Y, Paik I, Kim J-I, Oh E** (2019) Trehalose-6-phosphate signaling regulates
1012 thermoresponsive hypocotyl growth in *Arabidopsis thaliana.* EMBO Rep **20:** 47828
1013 **Ishihara H, Obata T, Sulpice R, Fernie AR, Stitt M** (2015) Quantitative determination of the rates of
1014 protein synthesis and turnover in Arabidopsis rosettes using dynamic $^{13}CO_2$ labelling and analysis
1015 of isotope enrichment of individual amino acids in free pools and in protein. Plant Physiol **168:**
1016 74-93
1017 **Ishihara H, Obata T, Sulpice R, Fernie AR, Stitt M** (2015) Quantifying protein synthesis and
1018 degradation in arabidopsis by dynamic $^{13}CO_2$ labeling and analysis of enrichment in individual
1019 amino acids in their free pools and in protein. Plant Physiol **168:** 74–93
1020 **Ishihara H, Moraes T, Pyl E-T, Schulze WX, Obata T, Scheffel A, Fernie AR, Sulpice R, Stitt M** (2017)
1021 Growth rate correlates negatively with protein turnover in Arabidopsis accessions. Plant J **91**:
1022 416-429
1023 **Ishihara H, Alseekh S, Feil R, et al.** (2022) Rising rates of starch degradation with time in the light and
1024 trehalose 6-phosphate levels optimize carbon availability and thereby buffer growth. Plant
1025 Physiol **189**: 1976-2000
1026 **Ivakov A, Flis A, Apelt F, et al.** (2017) Cellulose synthesis and cell expansion are regulated by different

1027 mechanisms in growing arabidopsis hypocotyls. Plant Cell **29:** 1305-1315
1028 **Jeong EY, Seo PJ, Woo JC, Park CM** (2015) AKIN10 delays flowering by inactivating IDD8 transcription
1029 factor through protein phosphorylation in Arabidopsis. BMC Plant Biol **15**: 1–13
1030 **Jossier M, Bouly JP, Meimoun P, Arjmand A, Lessard P, Hawley S, Hardie GD, Thomas M** (2009) SnRK1
1031 (SNF1-related kinase 1) has a central role in sugar and ABA signalling in *Arabidopsis thaliana*.
1032 Plant J **59**: 316–328
1033 **Kretzschmar T, Pelayo MAF, Trijatmiko KR, et al.** (2015) A trehalose-6-phosphate phosphatase
1034 enhances anaerobic germination tolerance in rice. Nat Plants **1:** 15124
1035 **Lastdrager J, Hanson J, Smeekens S** (2014) Sugar signals and the control of plant growth and
1036 development. J Exp Bot **65:** 799–807
1037 **Leyman B, van Dijck P, Thevelein JM** (2001) An unexpected plethora of trehalose biosynthesis genes
1038 in Arabidopsis thaliana. Trends Plant Sci **6:** 510–513
1039 **Locke JCW, Millar AJ, Turner MS** (2005) Modelling genetic networks with noisy and varied
1040 experimental data: the circadian clock in *Arabidopsis thaliana*. J Theor Biol **234**: 383–393
1041 **Lu C, Lin C, Lee K, Chen J, Huang L, Ho S, Liu H, Hsing Y, Yu S** (2007) The SnRK1A protein kinase plays
1042 a key role in sugar signaling during germination and seedling growth of rice. Plant Cell **19**: 2484–
1043 2499
1044 **Lunn JE, Feil R, Hendriks JHMM, et al.** (2006) Sugar-induced increases in trehalose 6-phosphate are
1045 correlated with redox activation of ADPglucose pyrophosphorylase and higher rates of starch
1046 synthesis in *Arabidopsis thaliana*. Biochem J **148**: 139–148
1047 **Lunn JE** (2007) Gene families and evolution of trehalose metabolism in plants. Funct Plant Biol **34**:
1048 550–563
1049 **Lunn JE, Delorge I, Mar C, van Dijck P, Stitt M** (2014) Trehalose metabolism in plants. Plant J **4**: 544–
1050 567
1051 **Lunn JE** (2016) Sucrose Metabolism. Encyclopedia of Life Sciences (ELS). John Wiley Sons, 1–9.
1052 **Ma J, Hanssen M, Lundgren K, et al.** (2011) The sucrose-regulated Arabidopsis transcription factor
1053 bZIP11 reprograms metabolism and regulates trehalose metabolism. New Phytol **191**: 733-745
1054 **Mair A, Pedrotti L, Wurzinger B, et al.** (2015) SnRK1-triggered switch of bZIP63 dimerization mediates
1055 the low-energy response in plants. Elife **4**: 05828
1056 **Margalha L, Confraria A** (2019) SnRK1 and TOR : modulating growth – defense trade-offs in plant
1057 stress responses. J Exp Bot **70:** 2261–2274
1058 **Martínez-Barajas E, Delatte T, Schluepmann H, et al.** (2011) Wheat grain development is
1059 characterized by remarkable trehalose 6-phosphate accumulation pregrain filling: tissue
1060 distribution and relationship to SNF1-related protein kinase1 activity. Plant Physiol **156**: 373–381

1061 **Martins MCM, Hejazi M, Fettke J, et al.** (2013) Feedback inhibition of starch degradation in
1062 arabidopsis leaves mediated by trehalose 6-phosphate. Plant Physiol **163**: 1142–1163
1063 **Mayer F V, Heath R, Underwood E, et al.** (2011) ADP regulates SNF1, the *Saccharomyces cerevisiae*
1064 homolog of AMP-activated protein kinase. Cell Metab **14**: 707–714
1065 **Mengin V, Pyl ET, Moraes TA, Sulpice R, Krohn N, Encke B, Stitt M** (2017) Photosynthate partitioning
1066 to starch in *Arabidopsis thaliana* is insensitive to light intensity but sensitive to photoperiod due
1067 to a restriction on growth in the light in short photoperiods. Plant Cell Environ **40**: 2608–2627
1068 **Millar AJ, Carré IA, Strayer CA, Chua NH, Kay SA** (1995) Circadian clock mutants in arabidopsis
1069 identified by luciferase imaging. Science **267**: 1161–1163
1070 **Moraes TA, Mengin V, Annunziata MG, Encke B, Krohn N, Höhne M, Stitt M** (2019) Response of the
1071 circadian clock and diel starch turnover to one day of low light or low CO_2. Plant Physiol **179**:
1072 1457–1478
1073 **Muralidhara P, Weiste C, Collani S, et al.** (2021) Perturbations in plant energy homeostasis prime
1074 lateral root initiation via SnRK1-bZIP63-ARF19 signalling. Proc Natl Acad Sci USA **118**: 210696111.
1075 **Murashige T, Skoog F** (1962) A revised medium for rapid growth and bio assays with tobacco tissue
1076 cultures. Physiol. Plant **15**: 473–497
1077 **Nietzsche M, Landgraf R, Tohge T, Börnke F** (2016) A protein-protein interaction network linking the
1078 energy-sensor kinase SnRK1 to multiple signaling pathways in *Arabidopsis thaliana*. Curr Opin
1079 Plant Biol **5**: 36–44
1080 **Nietzsche M, Schießl I, Börnke F, Griffiths CA** (2014) The complex becomes more complex : protein-
1081 protein interactions of SnRK1 with DUF581 family proteins provide a framework for cell- and
1082 stimulus type-specific SnRK1 signaling in plants. Front Plant Sci **5**: 1–13
1083 **Nuccio ML, Wu J, Mowers R, et al.** (2015) Expression of trehalose-6-phosphate phosphatase in maize
1084 ears improves yield in well-watered and drought conditions. Nat Biotech **33:** 862–869
1085 **Nukarinen E, Nägele T, Pedrotti L, Wurzinger B, Baena-González E, Dröge-Laser W, Weckwerth W**
1086 (2016) Quantitative phosphoproteomics reveals the role of the AMPK plant ortholog SnRK1 as a
1087 metabolic master regulator under energy deprivation. Sci Rep **6:** 31697
1088 **Nunes C, Hara LEO, Primavesi LF, et al.** (2013) The trehalose 6-phosphate/SnRK1 signaling pathway
1089 primes growth recovery following relief of sink limitation. Plant Physiol **162:** 1720–1732
1090 **Nunes C, Primavesi LF, Patel MK, Martinez-Barajas E, Powers SJ, Sagar R, Fevereiro PS, Davis BG,**
1091 **Paul MJ** (2013) Inhibition of SnRK1 by metabolites: Tissue-dependent effects and cooperative
1092 inhibition by glucose 1-phosphate in combination with trehalose 6-phosphate. Plant Physiol
1093 Biochem **63**: 89–98
1094 **Oszvald M, Primavesi LF, Grif A, Cohn J, Basu S, Nuccio ML, Paul MJ** (2018) Trehalose 6- phosphate

1095 regulates photosynthesis and assimilate partitioning in reproductive tissue. Plant Physiol **176:**
1096 2623–2638
1097 **Paul MJ, Gonzalez-Uriarte A, Grif CA, Hassani-Pak K** (2018) The role of trehalose 6-phosphate in crop
1098 yield and resilience. Plant Physiol **177:** 12–23
1099 **Paul MJ, Watson A, Griffiths CA** (2020) Trehalose 6-phosphate signalling and impact on crop yield.
1100 Biochem Soc Trans **48**: 2127-2137
1101 **Pedrotti L, Weiste C, Nägele T, et al.** (2018) Snf1-RELATED KINASE1-controlled C / S 1 -bZIP signaling
1102 activates alternative mitochondrial metabolic pathways to ensure plant survival in extended
1103 darkness. Plant Cell **30**: 495–509
1104 **Peixoto B, Moraes TA, Mengin V, et al.** (2021) Impact of the SnRK1 protein kinase on sucrose
1105 homeostasis and the transcriptome during the diel cycle. Plant Physiol **187**: 1357–1373
1106 **Piattoni CV, Bustos DM, Guerrero SA, Iglesias AÁ** (2011) Nonphosphorylating glyceraldehyde-3-
1107 phosphate dehydrogenase is phosphorylated in wheat endosperm at serine-404 by an SNF1-
1108 related protein kinase. Plant Physiol **156**: 1337–1350
1109 **Polge C, Jossier M, Crozet P, Gissot L, Thomas M** (2008) β-Subunits of the SnRK1 complexes share a
1110 common ancestral function together with expression and function specificities; physical
1111 interaction with nitrate reductase specifically occurs via AKINβ1-subunit. Plant Physiol **148**: 1570-
1112 1582
1113 **Polge C, Thomas M** (2006) SNF1 / AMPK / SnRK1 kinases, global regulators at the heart of energy
1114 control? Trends Plant Sci **12**: 20–28
1115 **Ponnu J, Wahl V, Schmid M** (2011) Trehalose-6-phosphate: Connecting plant metabolism and
1116 development. Front Plant Sci **2:** 70
1117 **Ramon M, Dang TVT, Broeckx T, Hulsmans S, Crepin N, Sheen J, Rolland F** (2019) Default activation
1118 and nuclear translocation of the plant cellular energy sensor SnRK1 regulate metabolic stress
1119 responses and development. Plant Cell **31:** 1614–1632
1120 **Randall RS** (2021) The plant AlcR-pAlcA ethanol-inducible system displays gross growth artefacts
1121 independently of downstream pAlcA-regulated inducible constructs. Sci Rep **11:** 1–5
1122 **Ryabova LA, Robaglia C, Meyer C** (2019) Target of Rapamycin kinase: central regulatory hub for plant
1123 growth and metabolism. J Exp Bot **70:** 2211-2216
1124 **Rodrigues A, Adamo M, Crozet P, et al.** (2013) ABI1 and PP2CA phosphatases are negative regulators
1125 of Snf1-related protein kinase1 signaling in Arabidopsis. Plant Cell **25:** 3871–3884
1126 **Ruiz-Gayosso A, Rodríguez-Sotres R, Martínez-Barajas E, Coello P** (2018) A role for the carbohydrate-
1127 binding module (CBM) in regulatory SnRK1 subunits: the effect of maltose on SnRK1 activity.
1128 Plant J **96:** 163–175

1129 **Sanagi M, Aoyama S, Kubo A, et al.** (2021) Low nitrogen conditions accelerate flowering by
1130 modulating the phosphorylation state of FLOWERING BHLH 4 in Arabidopsis. Proc Natl Acad Sci
1131 USA **118:** 2022942118
1132 **Sánchez-Villarreal A, Davis AM, Davis SJ** (2018) AKIN10 activity as a cellular link between metabolism
1133 and circadian-clock entrainment in *Arabidopsis thaliana*. Plant Signal Behav **13:** 1411448
1134 **Schluepmann H, Pellny T, van Dijken A, Smeekens S, Paul M** (2003) Trehalose 6-phosphate is
1135 indispensable for carbohydrate utilization and growth in *Arabidopsis thaliana*. Proc Natl Acad Sci.
1136 USA **100**: 6849–6854
1137 **Schluepmann H, Paul M** (2009) Trehalose metabolites in Arabidopsis—elusive, active and central.
1138 Arabidopsis Book **7:** 0122
1139 **Seki M, Ohara T, Hearn TJ, Frank A, da Silva VCH, Caldana C, Webb AAR, Satake A** (2017) Adjustment
1140 of the Arabidopsis circadian oscillator by sugar signalling dictates the regulation of starch
1141 metabolism. Sci Rep **7**: 8305
1142 **Sheen J, Baena-González E** (2008) Convergent energy and stress signaling. Trends Plant Sci **13:** 474-
1143 482
1144 **Shin J, Sánchez-Villarreal A, Davis AM, Du SX, Berendzen KW, Koncz C, Ding Z, Li C, Davis SJ** (2017)
1145 The metabolic sensor AKIN10 modulates the Arabidopsis circadian clock in a light-dependent
1146 manner. Plant Cell Environ **40:** 997–1008
1147 **Smith AM, Stitt M** (2007) Coordination of carbon supply and plant growth. Plant Cell Environ **30**:
1148 1126–1149
1149 **Stitt M, Wirtz W, Heldt HW** (1980) Metabolite levels during induction in the chloroplast and
1150 extrachloroplast compartments of spinach protoplasts. Biochim Biophys Acta Bioenerg **593**: 85–
1151 102
1152 **Sulpice R, Flis A, Ivakov AA, et al.** (2014) Arabidopsis coordinates the diurnal regulation of carbon
1153 allocation and growth across a wide range of photoperiods. Mol Plant **7**: 137–155
1154 **Toroser D, Plaut Z, Huber SC** (2000) Regulation of a plant SNF1-related protein kinase by glucose-6-
1155 phosphate. Plant Physiol **123:** 403–411
1156 **Usadel B, Bläsing OE, Gibon Y, Retzlaff K, Höhne M, Günther M, Stitt M** (2008) Global transcript levels
1157 respond to small changes of the carbon status during progressive exhaustion of carbohydrates
1158 in arabidopsis rosettes. Plant Physiol **146**: 1834–1861
1159 **Vandesteene L, Ramon M, Le K, van Dijck P, Rolland F** (2010) A single active trehalose-6-P synthase
1160 (TPS) and a family of putative regulatory TPS-like proteins in Arabidopsis. Mol Plant **3**: 406–419
1161 **Vandesteene L, López-Galvis L, Vanneste K, et al.** (2012) Expansive evolution of the *TREHALOSE-6-*
1162 *PHOSPHATE PHOSPHATASE* gene family in Arabidopsis. Plant Physiol **160**: 884–896

1163 **Wahl V, Ponnu J, Schlereth A, et al.** (2013) Regulation of flowering by trehalose-6-phosphate signaling
1164 in *Arabidopsis thaliana*. Science **339**: 704–707
1165 **Wang Y, Wang L, Micallef BJ, Tetlow IJ, Mullen RT, Feil R, Lunn JE, Emes MJ** (2020) AKINβ1, a subunit
1166 of SnRK1, regulates organic acid metabolism and acts as a global modulator of genes involved in
1167 carbon, lipid, and nitrogen metabolism. J Exp Bot **71**: 1010–1028
1168 **Wingler A, Delatte TL, Hara LEO, Primavesi LF, Jhurreea D, Paul MJ, Schluepmann H** (2012) Trehalose
1169 6-phosphate is required for the onset of leaf senescence associated with high carbon availability.
1170 Plant Physiol **158:** 1241–1251
1171 **Wurzinger B, Nukarinen E, Nägele T, Weckwerth W, Teige M** (2018) The SnRK1 kinase as central
1172 mediator of energy signaling between different organelles. Plant Physiol **176:** 1085–1094
1173 **Yang HL, Liu YJ, Wang CL, Zeng QY** (2012) Molecular evolution of trehalose-6-phosphate synthase
1174 (TPS) gene family in Populus, Arabidopsis and rice. PLoS One **7:** 42438
1175 **Zacharaki V, Ponnu J, Crepin N, Langenecker T, Hagmann J, Skorzinski N, Musialak-Lange M, Wahl**
1176 **V, Rolland F, Schmid M** (2022) Impaired KIN10 function restores developmental defects in the
1177 Arabidopsis *trehalose 6-phosphate synthase1* (*tps1*) mutant. New Phytol **235**: 220-233
1178 **Zhai Z, Liu H, Shanklin J** (2017) Phosphorylation of WRINKLED1 by KIN10 results in its proteasomal
1179 degradation, providing a link between energy homeostasis and lipid biosynthesis. Plant Cell **29**,
1180 871–889.
1181 **Zhai Z, Keereetaweep J, Liu H, Feil R, Lunn JE, Shanklin J** (2018) Trehalose 6- phosphate positively
1182 regulates fatty acid synthesis by stabilizing WRINKLED1. Plant Cell **30:** 2616–2627
1183 **Zhang Y, Primavesi LF, Jhurreea D, et al.** (2009) Inhibition of SNF1- related protein kinase1 activity
1184 and regulation of metabolic pathways by trehalose-6-phosphate. Plant Physiol **149**: 1860–1871
1185 **Zhang ZP, Deng Y, Song X, Miao M** (2015) Trehalose-6-phosphate and SNF1-related protein kinase 1
1186 are involved in the first-fruit inhibition of cucumber. J Plant Physiol **177**: 110–120
1187

1188 **Figure legends**

1189

1190 **Figure 1: Reproducible diel response in phosphorylation of SnRK1 reporters under equinoctial**
1191 **growth conditions.** SnRK1 reporter lines were grown in a 12-h photoperiod (irradiance 160 µmol m^{-2}
1192 s^{-1}) for 22 days as controls in three independent experiments, in which additional plants grown in
1193 parallel were subjected to different treatments (see Figs 2-4). Whole rosettes were harvested at 4-h
1194 intervals through the diel cycle. (A) Phosphorylation of the NUC/GEN polypeptide was quantified by
1195 immunoblotting as described in Methods and in Supplementary Figure S1. (B) Selected metabolites.
1196 Data are from the control samples from the following experiments: (i) Control 1: Supplementary
1197 Dataset S1 – Exp.3 (blue symbols; NUC and GEN lines); (ii) Control 2: Supplementary Dataset S1 – Exp.4
1198 and Supplementary Figure S4 (red symbols; NUC and GEN lines); (iii) Control 3: Supplementary Dataset
1199 S1 – Exp.2 and Supplementary Figure S3b (grey symbols; NUC line only). Data are shown as mean ±
1200 S.D. (n = 3-4 biological replicates, each containing 3-5 pooled rosettes). Statistical analyses are
1201 provided for each time series in Figs 2, 3 and 4, respectively.

1202

1203 **Figure 2: SnRK1 activity in Arabidopsis plants transferred to low irradiance for one light period.** NUC
1204 and GEN lines were grown in a 12-h photoperiod at 160 µmol m^{-2} s^{-1} irradiance for 19 days. At 20 DAS,
1205 starting at dawn (ZT0), irradiance was reduced to 60 µmol m^{-2} s^{-1} for the following 12 h (treatment
1206 light period), plants were darkened at ZT12 (treatment night), and at ZT24 were re-illuminated at an
1207 irradiance of 160 µmol m^{-2} s^{-1} (recovery day), as described in Moraes *et al*. (2019). Samples from both
1208 genotypes and from the corresponding control treatment (plants left in the original growth light
1209 regime) were harvested at 4-h intervals from ZT0-ZT36 (with respect to dawn on the treatment day).
1210 (A) Soluble sugars and starch. (B) Phosphorylation of NUC (top) and GEN (bottom) SnRK1 reporter
1211 polypeptides. The dashed grey background denotes the low-light treatment day. Results are shown as
1212 mean ± S.D. (n=3-4 biological replicates). Statistical analysis: letters indicate significant (P<0.05)
1213 changes between different times for a given genotype and asterisks indicate significant (P<0.05)
1214 differences between lines at a given time point, according to one-way ANOVA and pairwise multiple
1215 comparison post-testing using the Holm-Sidak method. The original and additional data are available
1216 in Supplementary Dataset S1 – Exp.3. The control time-series is also shown in Figure 1 (blue symbols).

1217

1218 **Figure 3: SnRK1 activity in Arabidopsis plants transferred to continuous low light.** NUC and GEN lines
1219 were grown in a 12-h photoperiod at 160 µmol m^{-2} s^{-1} irradiance for 19 days. At 20 DAS, plants were
1220 shifted at dawn (ZT0) to continuous low light (90 µmol m^{-2} s^{-1}) for 32 h, while corresponding controls

1221 were kept in the original growth conditions (12-h photoperiod, 160 µmol m^{-2} s^{-1}). (A) Diel changes of
1222 sugars and starch. (B) Phosphorylation of NUC (top) and GEN (bottom) SnRK1 reporter polypeptides.
1223 The dashed grey background represents the subjective night. Results are shown as mean ± S.D. (n = 3
1224 biological replicates). Statistical analysis: letters indicate significant (*P*<0.05) changes between
1225 different times for a given treatment and asterisks represent significant (*P*<0.05) differences between
1226 the low light treatment and the control at a given time point according to one-way ANOVA with
1227 pairwise multiple comparison post-testing using the Holm-Sidak method. The original and additional
1228 data are available in Supplementary Dataset S1 – Exp.4. The control time-series is also shown in Figure
1229 1 (red symbols).
1230
1231 **Figure 4: SnRK1 activity in Arabidopsis plants grown in T24 and T28 light-dark cycles.** NUC and GEN
1232 lines were grown from sowing in a 14-h light / 14 h dark (T28) cycle under 160 µmol m^{-2} s^{-1} irradiance
1233 for 19 days, in parallel with control plants that were grown in a 12-h light / 12-h dark (T24) cycle. At
1234 20 DAS (as defined by the T24 cycle), starting at dawn, plants were harvested at 4-h intervals
1235 throughout the light-dark cycle (open symbols). At the end of the light-dark cycle, additional plants
1236 were left in darkness and harvested for two further time points for the plants grown in a T24 cycle (i.e.
1237 at ZT28 and ZT32), and for one further time point for plants grown in a T28 cycle (i.e. at ZT32). (A)
1238 Soluble sugars and starch. (B) Phosphorylation of NUC (top) and GEN (bottom) SnRK1 reporter
1239 polypeptides. The white background represents light in both T cycles and the grey shaded areas
1240 represent darkness (ZT12-ZT24 for the T24 cycle and ZT14-ZT28 for the T28 cycle) in one or both T
1241 cycles: pale grey denotes darkness in the T24 and light in the T28 cycle, mid-grey denotes darkness in
1242 both T-cycles, and dark grey represents extended night in both T cycles. Black closed symbols
1243 represent time points in extended darkness. Results are shown as mean ± S.D. (n = 3 biological
1244 replicates). Statistical analysis: letters indicate significant (*P*<0.05) changes between different times
1245 for a given genotype and asterisks represent significant (*P*<0.05) differences between T28 vs T24 at a
1246 given time point according to a one-way ANOVA with pairwise multiple comparison post-testing using
1247 the Holm-Sidak method. The original and additional data are available in Supplementary Dataset S1-
1248 Exp.5. The control time-series is also shown in Figure 1 (grey symbols).
1249
1250 **Figure 5: Elevated Tre6P in the light period inhibits nuclear SnRK1 activity.** Line #6.3 (NUC x iTPS) was
1251 grown in a 12-h photoperiod at 160 µmol m^{-2} s^{-1} irradiance for 20 days. At 21 DAS, plants were sprayed
1252 at ZT4 (red arrow) with 2% (v/v) ethanol to induce the expression of bacterial TPS (otsA) or with water
1253 as a mock-induction control, and then harvested at ZT7, ZT9 and ZT11 for measurement of Tre6P (top
1254 panel), sucrose (middle) and the phosphorylation status of the NUC polypeptide (bottom) as a readout

1255 of nuclear SnRK1 activity *in vivo*. Results are shown as mean ± S.D. (n = 3-4 biological replicates).
1256 Statistical analysis: asterisks indicate significant (P<0.05) differences between the ethanol-induced
1257 plants and water controls according to a one-way ANOVA with pairwise multiple comparison post-
1258 testing using the Holm-Sidak method. Additional metabolites are shown in Supplementary Figure S7.
1259 The original data are available in Supplementary Dataset S1 – Exp.7.
1260
1261 **Figure 6: Transiently high Tre6P at the end of the night leads to an increase in nuclear SnRK1 activity.**
1262 Line #6.3 (NUC x iTPS) and #1.2 control (NUC x alcR) were grown in short-day conditions (6 h light / 18
1263 h dark) at 160 µmol m^{-2} s^{-1} irradiance for 25 days. At 26 DAS, plants were sprayed with 2% (v/v) ethanol
1264 at ZT20 (red arrow) to induce the expression of bacterial TPS (otsA). Rosettes were harvested at ZT20,
1265 ZT22 and ZT24 (end of normal night), and at ZT25 and ZT27 (extended darkness)for measurement of:
1266 Tre6P (top panel) and the phosphorylation of the NUC polypeptide (bottom) as a readout of nuclear
1267 SnRK1 activity *in vivo*. Results are shown as mean ± S.D. (n=3-4 biological replicates). Statistical
1268 analysis: letters indicate significant (P<0.05) changes between different times for a given genotype
1269 and asterisks indicate significant (P<0.05) differences between the #6.3 (NUC x iTPS) and #1.2 control
1270 (NUC x alcR) lines according to a one-way ANOVA with pairwise multiple comparison post-testing using
1271 the Holm-Sidak method. Additional metabolites are shown in Supplementary Figure S8. The original
1272 data are available in Supplementary Dataset S1 – Exp.7.
1273

1274 **Table 1: Correlation between metabolite levels and NUC or GEN phosphorylation.** Presented are R^2
1275 and p-values of linear regression, performed separately for the three independent control
1276 experiments compiled in Figure 1. Linear regression analysis was performed with the "least squares"
1277 method, using individual replicates for the complete diel cycle (ZT0 to ZT24). The column +/- provides
1278 information about the slope of the regression: positive (+), negative (-). Significant correlations ($p <$
1279 0.05) are highlighted in blue (positive) or red (negative). n.d. not determined. Individual plots are
1280 provided in Supplementary Dataset S2.

Experiment	Metabolite	NUC			GEN		
		R^2	p-value	+/-	R^2	p-value	+/-
1	Tre6P	0.007	0.673	+	0.001	0.965	+
	Glc6P	0.048	0.270	-	**0.225**	**0.030**	-
	Glc1P	0.056	0.236	-	0.036	0.412	-
	Starch	0.006	0.706	+	0.051	0.324	-
	Sucrose	0.085	0.139	-	0.058	0.295	-
	Glucose	0.121	0.076	+	**0.272**	**0.015**	+
2	Tre6P	0.004	0.778	+	0.046	0.325	-
	Glc6P	**0.215**	**0.022**	-	**0.583**	**2.24×10^{-5}**	-
	Glc1P	**0.418**	**0.001**	-	**0.683**	**1.17×10^{-6}**	-
	Starch	0.081	0.190	-	0.081	0.189	-
	Sucrose	1×10^{-8}	0.685	-	**0.324**	**0.005**	-
	Glucose	0.054	0.687	-	2×10^{-5}	0.985	-
3	Tre6P	0.004	0.233	-	n.d.	n.d.	
	Glc6P	0.002	0.766	-	n.d.	n.d.	
	Glc1P	0.02	0.373	+	n.d.	n.d.	
	Starch	0.032	0.364	-	n.d.	n.d.	
	Sucrose	0.007	0.678	+	n.d.	n.d.	
	Glucose	0.013	0.561	-	n.d.	n.d.	

1281

A.

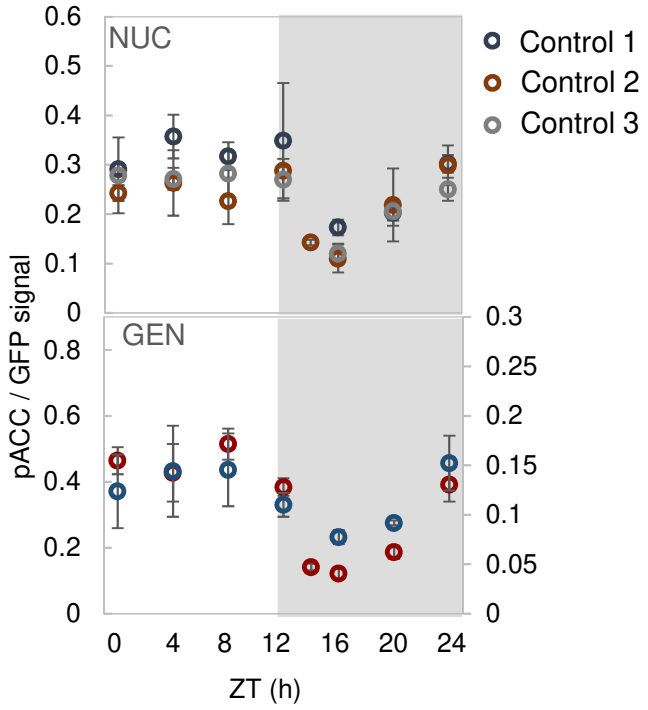

B.

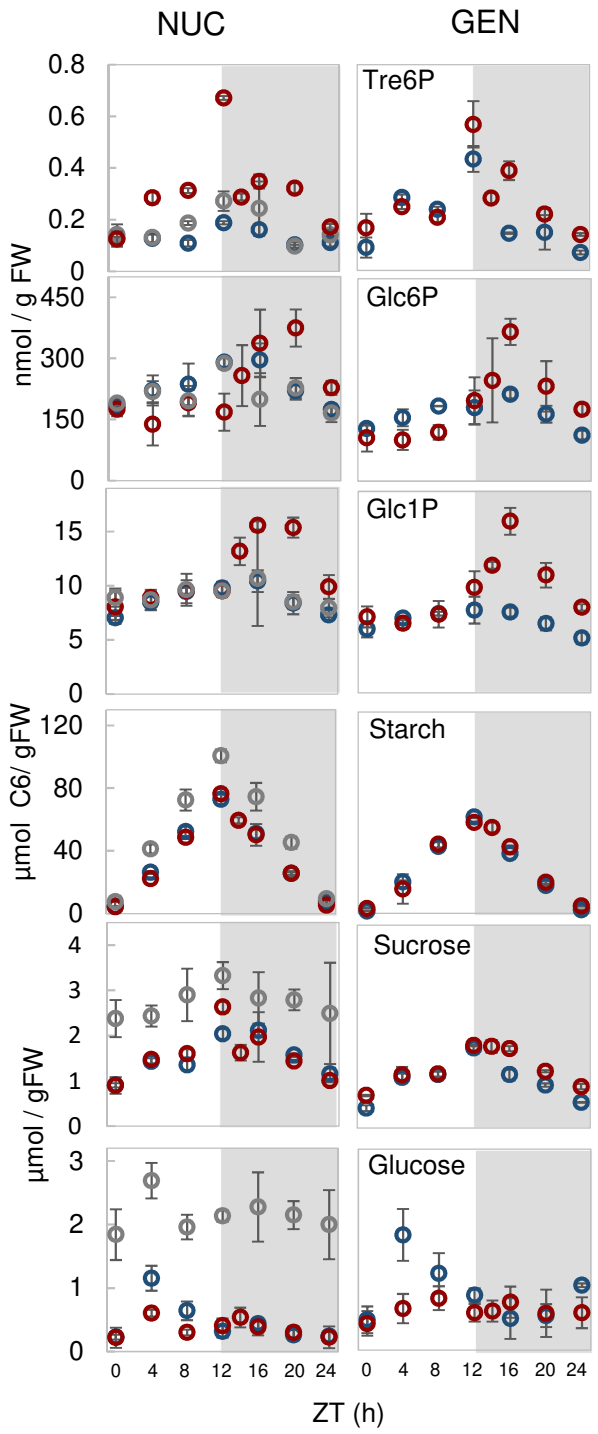

Figure 1: Reproducible diel response in phosphorylation of SnRK1 reporters under equinoctial growth conditions. SnRK1 reporter lines were grown in a 12-h photoperiod (irradiance 160 µmol m^{-2} s^{-1}) for 22 days as controls in three independent experiments, in which additional plants grown in parallel were subjected to different treatments (see Figs 2-4). Whole rosettes were harvested at 4-h intervals through the diel cycle. (A) Phosphorylation of the NUC/GEN polypeptide was quantified by immunoblotting as described in Methods and in Supplementary Figure S1. (B) Selected metabolites. Data are from the control samples from the following experiments: (i) Control 1: Supplementary Dataset S1 – Exp.3 (blue symbols; NUC and GEN lines); (ii) Control 2: Supplementary Dataset S1 – Exp.4 and Supplementary Figure S4 (red symbols; NUC and GEN lines); (iii) Control 3: Supplementary Dataset S1 – Exp.2 and Supplementary Figure S3b (grey symbols; NUC line only). Data are shown as mean ± S.D. (n = 3-4 biological replicates, each containing 3-5 pooled rosettes). Statistical analyses are provided for each time series in Figs 2, 3 and 4, respectively.

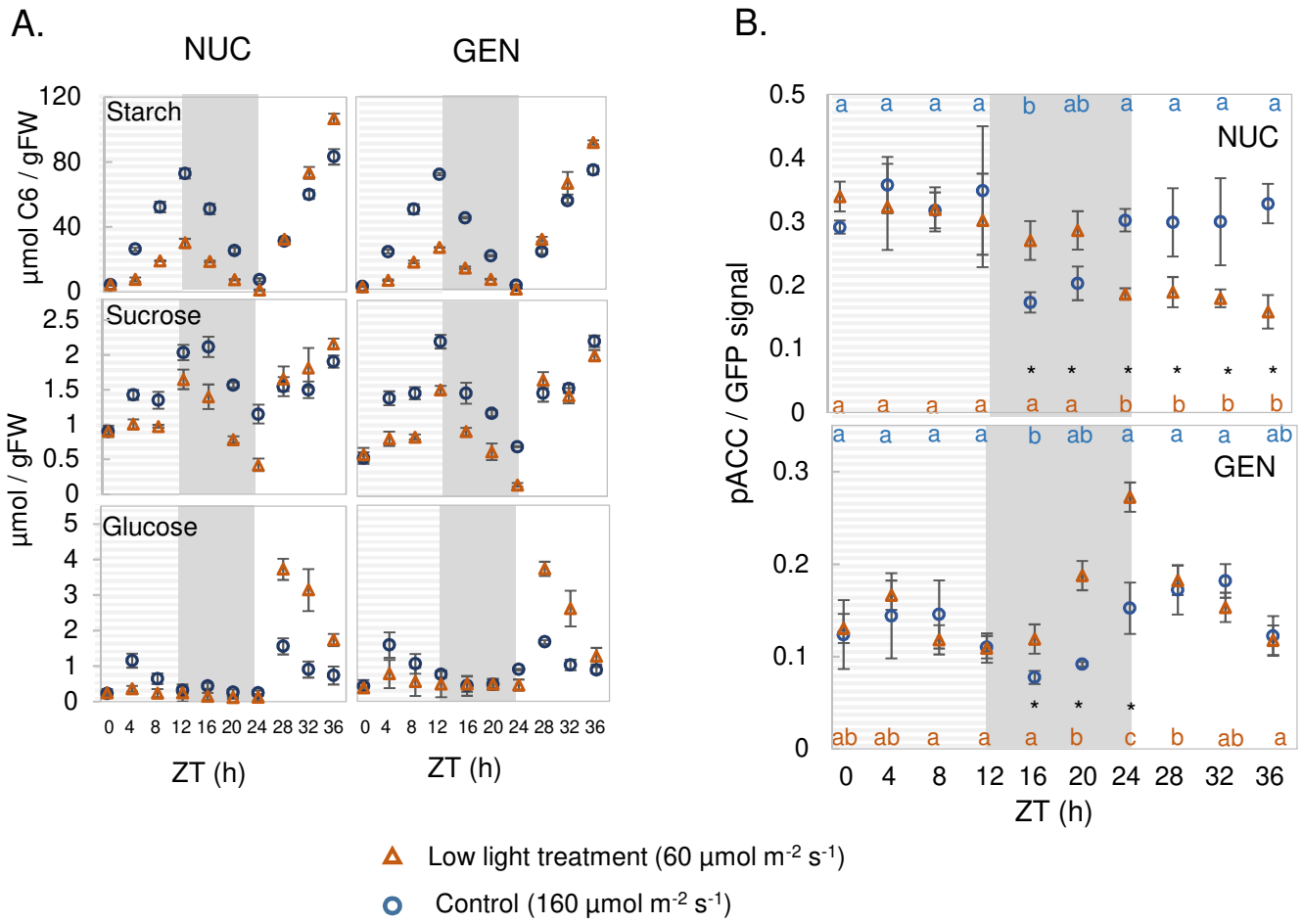

Figure 2: SnRK1 activity in Arabidopsis plants transferred to low irradiance for one light period. NUC and GEN lines were grown in a 12-h photoperiod at 160 µmol m^{-2} s^{-1} irradiance for 19 days. At 20 DAS, starting at dawn (ZT0), irradiance was reduced to 60 µmol m^{-2} s^{-1} for the following 12 h (treatment light period), plants were darkened at ZT12 (treatment night), and at ZT24 were re-illuminated at an irradiance of 160 µmol m^{-2} s^{-1} (recovery day), as described in Moraes *et al*. (2019). Samples from both genotypes and from the corresponding control treatment (plants left in the original growth light regime) were harvested at 4-h intervals from ZT0-ZT36 (with respect to dawn on the treatment day). (A) Soluble sugars and starch. (B) Phosphorylation of NUC (top) and GEN (bottom) SnRK1 reporter polypeptides. The dashed grey background denotes the low-light treatment day. Results are shown as mean ± S.D. (n=3-4 biological replicates). Statistical analysis: letters indicate significant (P<0.05) changes between different times for a given genotype and asterisks indicate significant (P<0.05) differences between lines at a given time point, according to one-way ANOVA and pairwise multiple comparison post-testing using the Holm-Sidak method. The original and additional data are available in Supplementary Dataset S1 – Exp.3. The control time-series is also shown in Figure 1 (blue symbols).

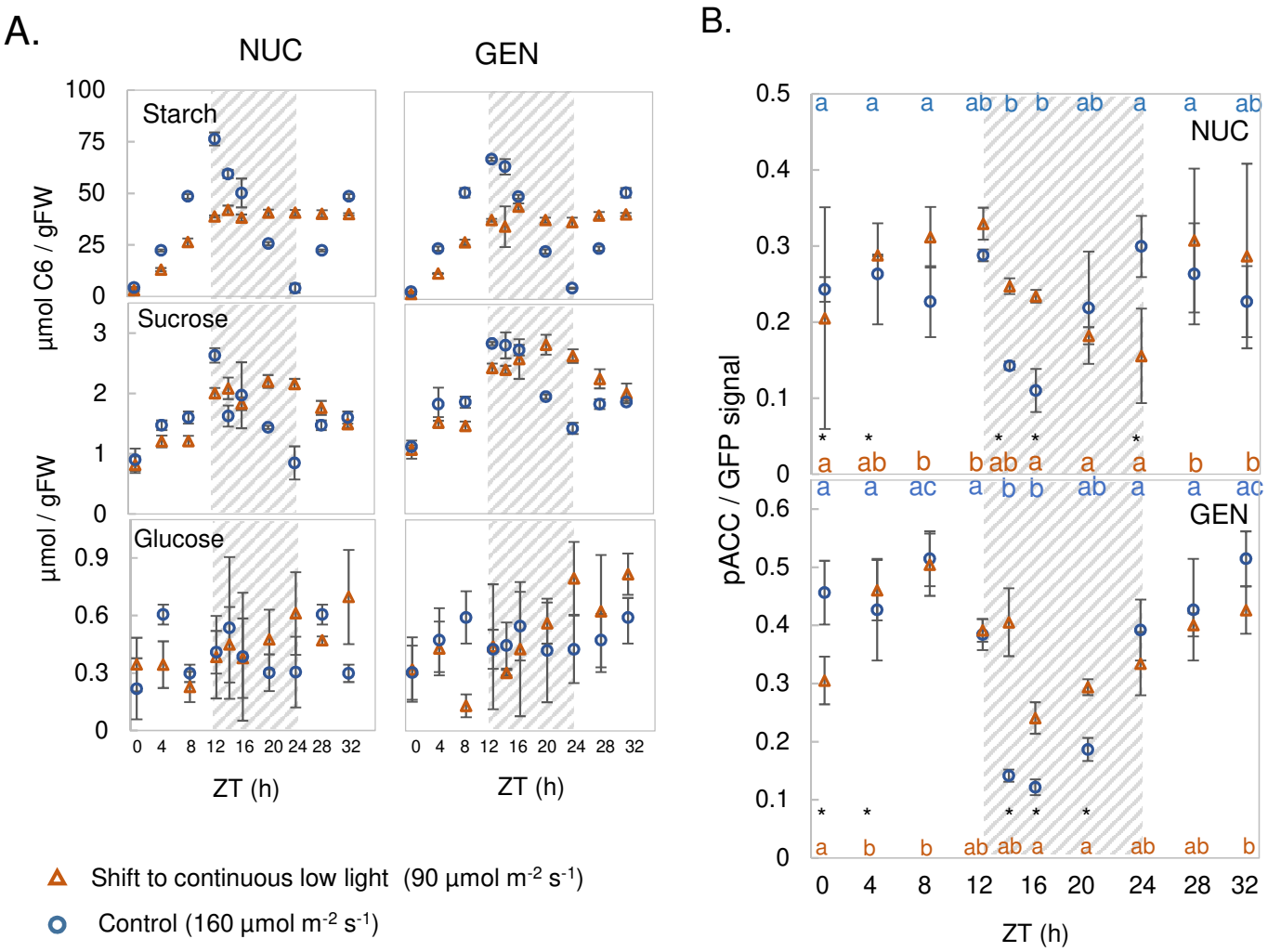

Figure 3: SnRK1 activity in Arabidopsis plants transferred to continuous low light. NUC and GEN lines were grown in a 12-h photoperiod at 160 µmol m^{-2} s^{-1} irradiance for 19 days. At 20 DAS, plants were shifted at dawn (ZT0) to continuous low light (90 µmol m^{-2} s^{-1}) for 32 h, while corresponding controls were kept in the original growth conditions (12-h photoperiod, 160 µmol m^{-2} s^{-1}). (A) Diel changes of sugars and starch. (B) Phosphorylation of NUC (top) and GEN (bottom) SnRK1 reporter polypeptides. The dashed grey background represents the subjective night. Results are shown as mean ± S.D. (n = 3 biological replicates). Statistical analysis: letters indicate significant (P<0.05) changes between different times for a given treatment and asterisks represent significant (P<0.05) differences between the low light treatment and the control at a given time point according to one-way ANOVA with pairwise multiple comparison post-testing using the Holm-Sidak method. The original and additional data are available in Supplementary Dataset S1 – Exp.4. The control time-series is also shown in Figure 1 (red symbols).

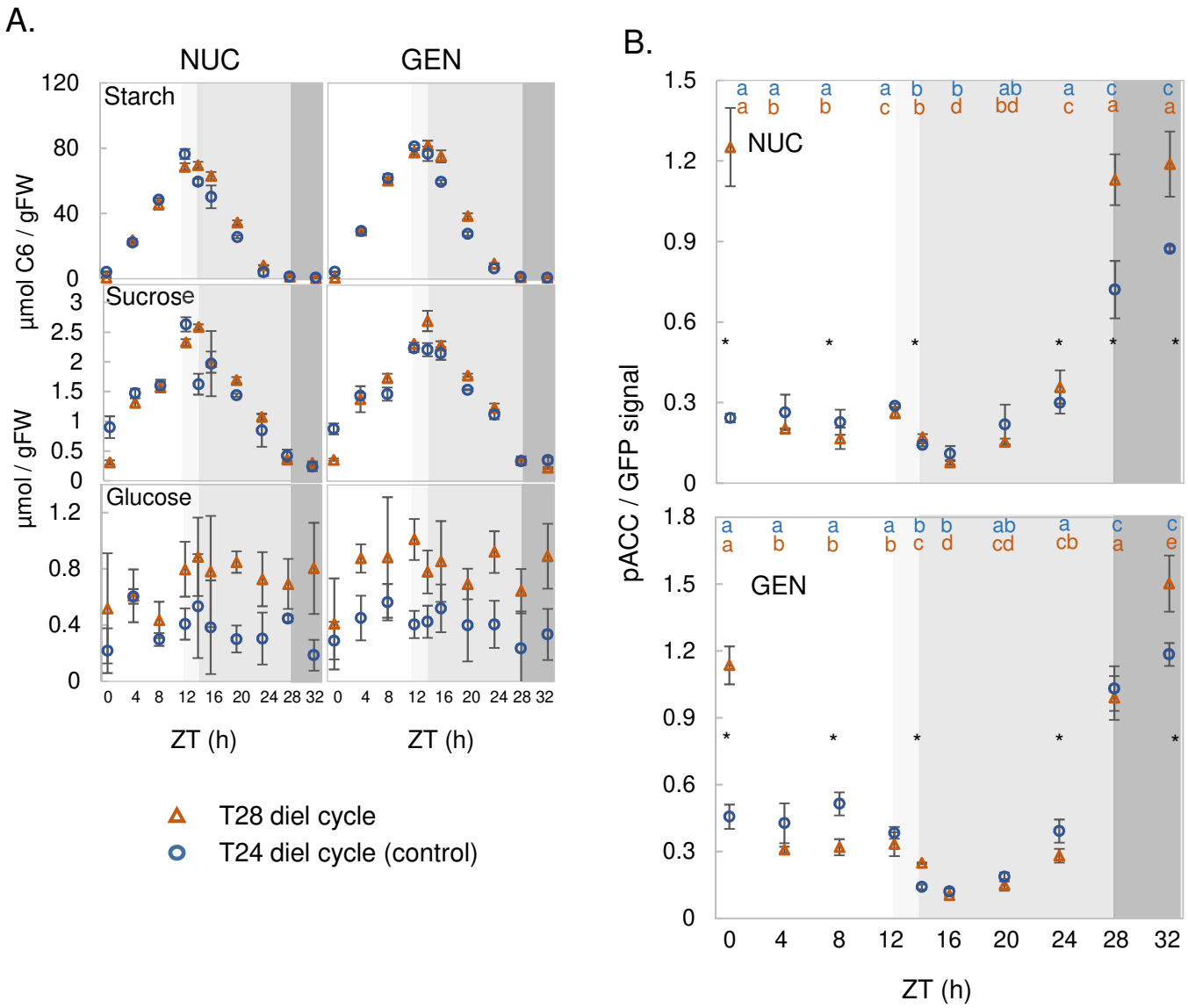

Figure 4: SnRK1 activity in Arabidopsis plants grown in T24 and T28 light-dark cycles. NUC and GEN lines were grown from sowing in a 14-h light / 14 h dark (T28) cycle under 160 µmol m^{-2} s^{-1} irradiance for 19 days, in parallel with control plants that were grown in a 12-h light / 12-h dark (T24) cycle. At 20 DAS (as defined by the T24 cycle), starting at dawn, plants were harvested at 4-h intervals throughout the light-dark cycle (open symbols). At the end of the light-dark cycle, additional plants were left in darkness and harvested for two further time points for the plants grown in a T24 cycle (i.e. at ZT28 and ZT32), and for one further time point for plants grown in a T28 cycle (i.e. at ZT32). (A) Soluble sugars and starch. (B) Phosphorylation of NUC (top) and GEN (bottom) SnRK1 reporter polypeptides. The white background represents light in both T cycles and the grey shaded areas represent darkness (ZT12-ZT24 for the T24 cycle and ZT14-ZT28 for the T28 cycle) in one or both T cycles: pale grey denotes darkness in the T24 and light in the T28 cycle, mid-grey denotes darkness in both T-cycles, and dark grey represents extended night in both T cycles. Black closed symbols represent time points in extended darkness. Results are shown as mean ± S.D. (n = 3 biological replicates). Statistical analysis: letters indicate significant (P<0.05) changes between different times for a given genotype and asterisks represent significant (P<0.05) differences between T28 vs T24 at a given time point according to a one-way ANOVA with pairwise multiple comparison post-testing using the Holm-Sidak method. The original and additional data are available in Supplementary Dataset S1- Exp.5. The control time-series is also shown in Figure 1 (grey symbols).

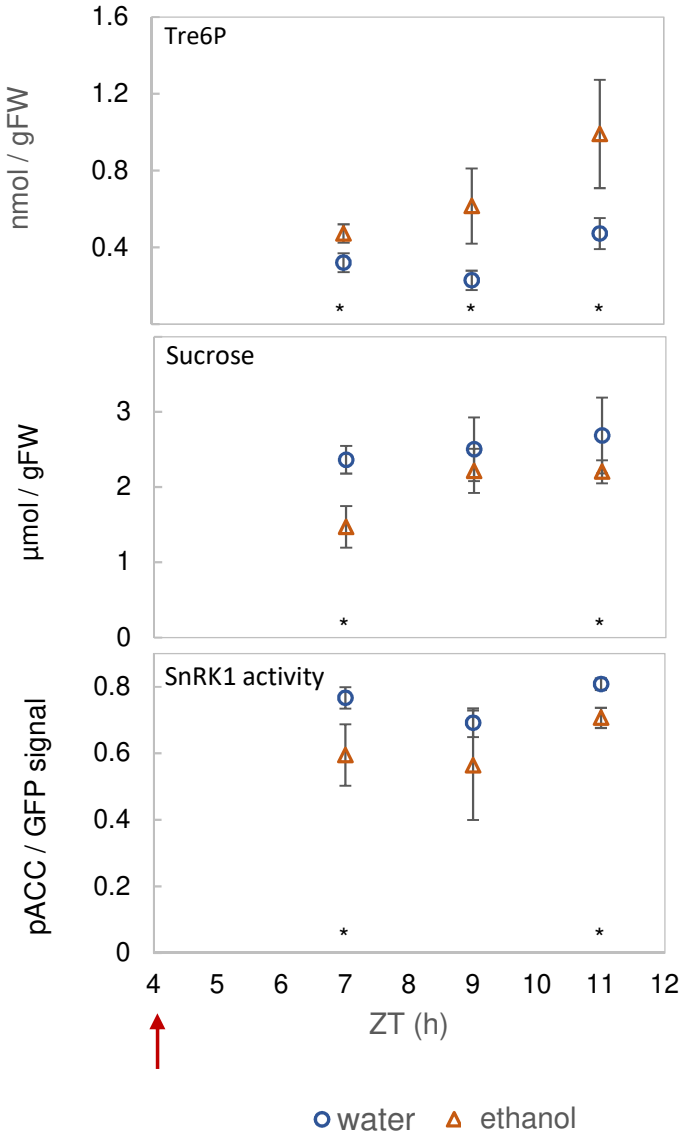

Figure 5: Elevated Tre6P in the light period inhibits nuclear SnRK1 activity. Line #6.3 (NUC x iTPS) was grown in a 12-h photoperiod at 160 µmol m^{-2} s^{-1} irradiance for 20 days. At 21 DAS, plants were sprayed at ZT4 (red arrow) with 2% (v/v) ethanol to induce the expression of bacterial TPS (otsA) or with water as a mock-induction control, and then harvested at ZT7, ZT9 and ZT11 for measurement of Tre6P (top panel), sucrose (middle) and the phosphorylation status of the NUC polypeptide (bottom) as a readout of nuclear SnRK1 activity *in vivo*. Results are shown as mean ± S.D. (n = 3-4 biological replicates). Statistical analysis: asterisks indicate significant (P<0.05) differences between the ethanol-induced plants and water controls according to a one-way ANOVA with pairwise multiple comparison post-testing using the Holm-Sidak method. Additional metabolites are shown in Supplementary Figure S7. The original data are available in Supplementary Dataset S1 – Exp.7.

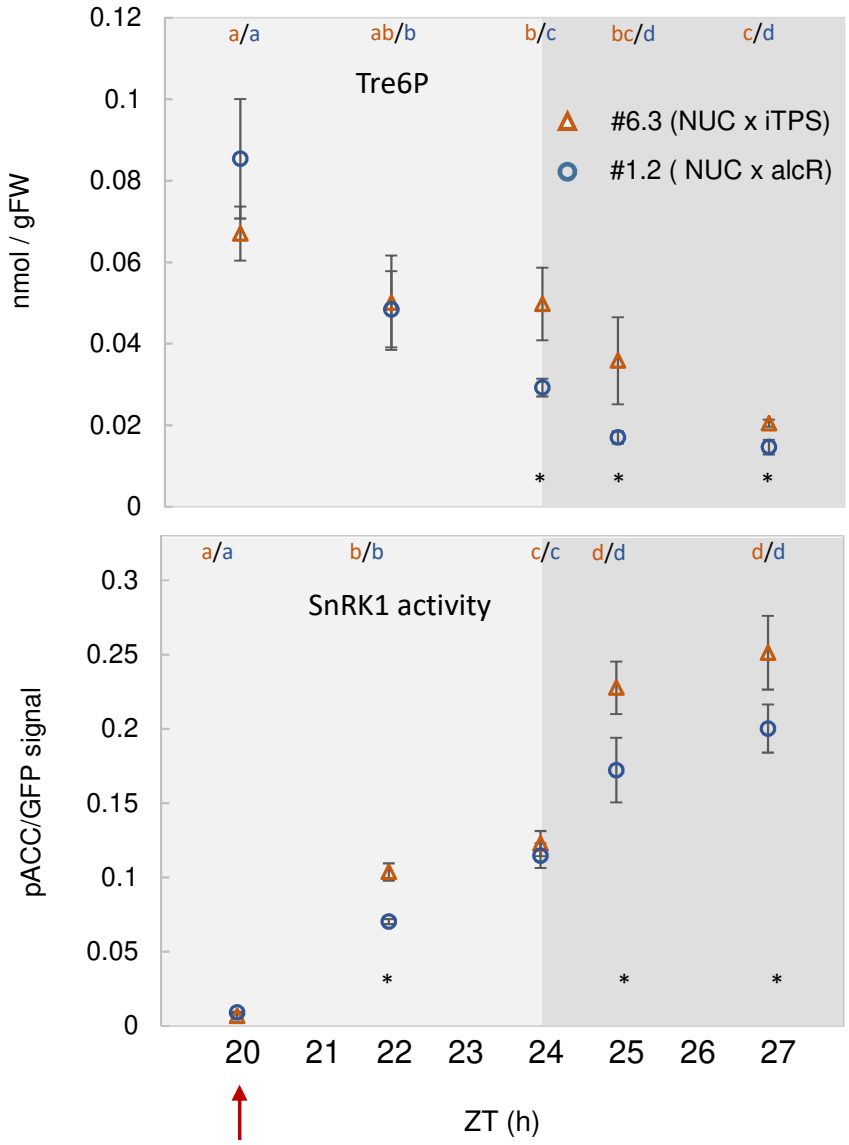

Figure 6: Transiently high Tre6P at the end of the night leads to an increase in nuclear SnRK1 activity. Line #6.3 (NUC x iTPS) and #1.2 control (NUC x alcR) were grown in short-day conditions (6 h light / 18 h dark) at 160 µmol m^{-2} s^{-1} irradiance for 25 days. At 26 DAS, plants were sprayed with 2% (v/v) ethanol at ZT20 (red arrow) to induce the expression of bacterial TPS (otsA). Rosettes were harvested at ZT20, ZT22 and ZT24 (end of normal night), and at ZT25 and ZT27 (extended darkness)for measurement of: Tre6P (top panel) and the phosphorylation of the NUC polypeptide (bottom) as a readout of nuclear SnRK1 activity *in vivo*. Results are shown as mean ± S.D. (n=3-4 biological replicates). Statistical analysis: letters indicate significant (P<0.05) changes between different times for a given genotype and asterisks indicate significant (P<0.05) differences between the #6.3 (NUC x iTPS) and #1.2 control (NUC x alcR) lines according to a one-way ANOVA with pairwise multiple comparison post-testing using the Holm-Sidak method. Additional metabolites are shown in Supplementary Figure S8. The original data are available in Supplementary Dataset S1 – Exp.7.